Polymers **2013**, *5*, 527-575; doi:10.3390/polym5020527

OPEN ACCESS

polymers

ISSN 2073-4360

www.mdpi.com/journal/polymers

Review

Structural Diversity of Metallosupramolecular Assemblies Based on the Bent Bridging Ligand 4,4′-Dithiodipyridine †

Rüdiger W. Seidel [1,*], Richard Goddard [2] and Iris M. Oppel [3]

[1] Lehrstuhl für Analytische Chemie, Ruhr-Universität Bochum, Universitätsstraße 150, Bochum 44780, Germany

[2] Max-Planck-Institut für Kohlenforschung, Kaiser-Wilhelm-Platz 1, Mülheim an der Ruhr 45470, Germany; E-Mail: goddard@mpi-muelheim.mpg.de

[3] Institut für Anorganische Chemie, Rheinisch-Westfälische Technische Hochschule Aachen, Landoltweg 1, Aachen 52074, Germany; E-Mail: iris.oppel@ac.rwth-aachen.de

† In memoriam Dr. Ulrich Siering (1957–2012).

* Author to whom correspondence should be addressed; E-Mail: ruediger.seidel@rub.de; Tel.: +49-241-8094-649; Fax: +49-241-8092-644.

Received: 2 April 2013; in revised form: 30 April 2013 / Accepted: 3 May 2013 / Published: 21 May 2013

Abstract: 4,4′-Dithiodipyridine (**dtdp**), also termed 4,4′-dipyridyldisulfide, is a bridging ligand of the 4,4′-bipyridine type. The introduction of the disulfide moiety inevitably leads to a relatively rigid angular structure, which exhibits axial chirality. More than 90 metal complexes containing the **dtdp** ligand have been crystallographically characterised until now. This review focuses on the preparation and structural diversity of discrete and polymeric metallosupramolecular assemblies constructed from **dtdp** as bridging ligands. These encompass metallamacrocycles with M_2L_2 topology and coordination polymers with periodicity in one or two dimensions. One-dimensional coordination polymers represent the vast majority of the metallosupramolecular structures obtained from **dtdp**. These include repeated rhomboids, zigzag, helical and arched chains among other types. In this contribution, we make an attempt to provide a comprehensive account of the structural data that are currently available for metallosupramolecular assemblies based on the bent bridging ligand **dtdp**.

Keywords: self-assembly; metallamacrocycle; coordination polymer; crystal engineering; 4,4′-dithiodipyridine; 4,4′-dipyridyldisulfide

1. Introduction and Scope

In metallosupramolecular chemistry, the fundamental building blocks are metal ions and usually organic bridging ligands capable of linking at least two metal ions in a divergent fashion [1–3]. Depending on the nature of the complementary building blocks and the reaction conditions, metallosupramolecular self-assembly can result in discrete or polymeric structures; the latter are broadly referred to as coordination polymers [4]. There has been an immense increase in research activity in the field since the early 1990s. This has at least in part been aided by advancements in analytical methods, such as the advent of area detectors for single-crystal X-ray diffraction, which has expedited characterisation. Metallosupramolecular chemistry also offers the promise of novel materials with interesting properties. Discrete metallosupramolecular assemblies, e.g., metallamacrocycles, box and cage compounds, have been used, for example, as receptors and reaction containers [5–10]. Potential applications in catalysis, gas-storage, separation, sensing, magnetism, optics and electrochemistry have often been mentioned in connection with coordination polymers [11–17]. The directional-bonding approach to the synthesis of discrete metallosupramolecular compounds with well-defined shape exploits the combination of rigid, multibranched ligands (L) with highly directional coordinating groups and geometrically preconfigured metal ions (M) [18]. A related net-based approach to crystal engineering of coordination polymers has been developed [19].

The pyridyl group is one of the most widely used coordinating groups within the directional-bonding approach to the synthesis of discrete metallosupramolecular assemblies and the net-based approach to coordination polymers. 4,4′-Dithiodipyridine (**dtdp**), also termed 4,4′-dipyridyldisulfide, is an *N*,*N*′-bridging ligand of the 4,4′-bipyridine family of bridging ligands. It is structurally related to 1,2-bis(4-pyridyl)ethane. The effect of the non-alkyl spacer linking the two pyridyl groups is, however, crucial to the molecular structure, since whereas in 1,2-bis(4-pyridyl)ethane the pyridyl groups can adopt the *anti* or *gauche* conformation about the ethylene group (Figure 1a), **dtdp** is only found in the *gauche* conformation. It is thus a relatively rigid angular bridging ligand with an almost ideal 90° bend angle. In the *gauche* conformation, the molecule exhibits axial chirality, resulting in conformational enantiomers [20]. The left-handed *M* form and the right-handed *P* form are shown in Figure 1b. The two forms exist in an equilibrium mixture in solution, since the barrier of rotation is relatively low [21]. The **dtdp** ligand has the additional feature that the disulfide functional group has a tendency for oxidative or reductive bond cleavage. Whether intentionally or not, S–S and C–S cleavage and rearrangement reactions of **dtdp** can lead to *in situ* formation of, for example, pyridine-4-thiolate, pyridine-4-sulfonate, the corresponding monosulfide and trisulfide, which in turn can act as ligands or counter-ions in the final outcome. Although we shall occasionally address the *in situ* formation of cleavage products of **dtdp** in connection with coordination polymers, cleavage reactions of the ligand are not subject of this review. The interested reader is directed to a recent review by Zhu and Gou [22].

We should add that we have even observed sulfate ions in crystalline products as a result of oxidative decomposition of **dtdp** after prolonged standing of the crystallisation mixture at ambient conditions [23].

Figure 1. (**a**) Schematic drawing of the *anti* and *gauche* conformers of 1,2-bis(4-pyridyl)ethane; (**b**) Illustration of the two *gauche* conformational enantiomers of **dtdp**: left-handed *M* form and right-handed *P* form.

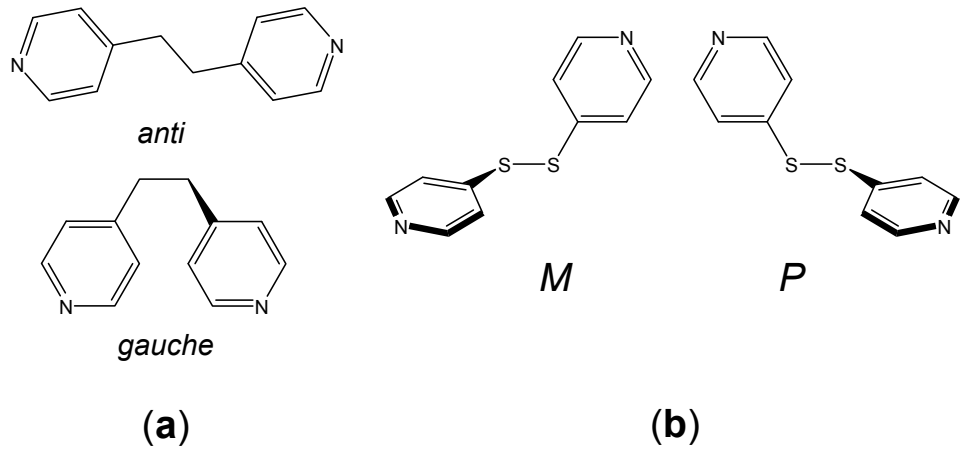

In their 2006 review of metallosupramolecular complexes derived from **dtdp**, Horikoshi and Mochida reasoned that molecular ML and ML_2 complexes of **dtdp** (Figure 2) were difficult to isolate, because asymmetric disulfides tend to disproportionate into symmetric ones in solution [24]. To the best of our knowledge, ML complexes have not been described so far, but a few ML_2 complexes have been obtained with Mn(II) [25], Cu(II) [26] and Zn(II) [27]. Furthermore, a one-dimensional Cd(II) coordination polymer containing μ-bridging and terminal **dtdp** in coexistence has been described [28] (CSD Refcode: INIMEY, see Section 3.3). Mononuclear ML_2 complexes will not be described in more detail in this review. The same holds for dinuclear M_2L complexes with a single **dtdp** linkage, which have been derived from Co(III) [29], Ru(II) [30,31], Ir(III) [31] so far. Thirty five structures of metallamacrocycles and coordination polymers are listed in Horikoshi and Mochida's review of 2006. Meanwhile, the number of relevant structures that can be found in the literature has increased to about 90. In this contribution, we attempt to provide an up-to-date and comprehensive account of the structural data that are currently available for metallamacrocycles and coordination polymers containing the bent bridging ligand **dtdp**.

Figure 2. Schematic representation of molecular **dtdp** complexes. Large grey spheres represent metal units.

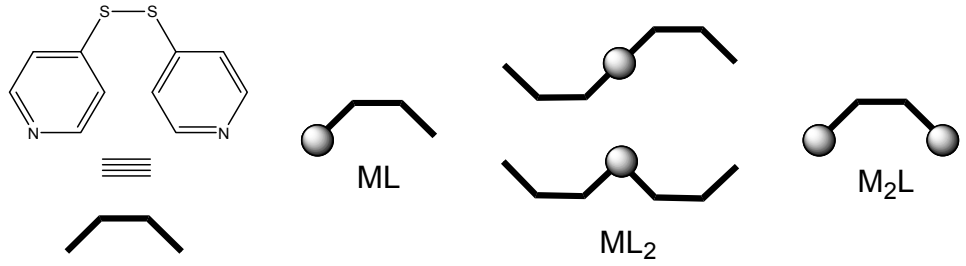

2. Methods

Structural data were taken from the Cambridge Structural Database (CSD) [32,33]. In order to include the most recent additions to the database, a search with the WebCSD interface [34] was carried out in January 2013. For the sake of easy reference, each structure in this review is referred to by its CSD Refcode, except those that have not yet been included in the CSD. Representations of crystal and molecular structures were drawn with Mercury 3.1 [35,36]. For coordination polymers, the pictures show various truncated parts, usually containing several repeat units. Carbon-bound hydrogen atoms, counter-ions and solvent molecules are omitted for clarity, unless otherwise indicated. Structural parameters were calculated geometrically on the basis of the atomic coordinates, using Mercury 3.1. (S–S)···(S–S) distances are based on the midpoints of the disulfide bonds. Concerning the C–S–S–C torsion angles reported in this work: unless the structure contains two crystallographically distinct **dtdp** ligands, positive torsion angles (*i.e.*, those of the right-handed *P* form) are given throughout for centrosymmetric crystal structures, although the asymmetric unit chosen in the original work may contain the left-handed *M* form. Solvent-accessible voids in the structures were also calculated with Mercury 3.1 (probe radius 1.2 Å, grid spacing 0.2 Å).

3. Structural Classification

The **dtdp** containing metallosupramolecular compounds in this review have been classified according to the topologies of the structures in the solid-state. This approach seems to be more appropriate than a classification by the nature of the metal units or reaction conditions, such as the solvents used in the supramolecular synthesis [37], since it is often the topologies that are of interest. When appropriate, cross-references are made. Figure 3 depicts some basic structural motifs found in metallosupramolecular assemblies derived from **dtdp**. For the sake of consistency, the labelling scheme has been adapted from the review by Horikoshi and Mochida [24]. Before we go into details, some clarification of the terminology used seems to be in order. We are not aware of a strict definition of what comprises a discrete metallosupramolecular species and the borderline between molecular and supramolecular coordination chemistry is blurred. It seems to be generally accepted, however, that macrocycles, boxes, cages and other higher order structures constructed from metal units and bridging ligands are labelled metallosupramolecular. In this sense, macrocycles with M_2L_2 topology, *i.e.*, two metal units joined by two **dtdp** ligands, are, as far as we can ascertain, the only discrete structurally characterised metallosupramolecular compounds that have been obtained with **dtdp** so far. Provisional recommendations on coordination polymer terminology by the International Union of Pure and Applied Chemistry (IUPAC) are currently in preparation [38]. Accordingly, a coordination polymer is a coordination compound continuously extending in one, two or three dimensions. Coordination networks have been defined as a subset of coordination polymers and represent either one-dimensional coordination polymers with cross-links between two or more individual chains, loops or spiro-links, or two- or three-dimensional coordination polymers. Following these definitions, **dtdp** containing structures with repeated rhomboid, necklace and tubular chain, as well as the (4,4) net topology, may be labeled as coordination networks, whereas helical, arched and zigzag chains belong to the group of pure one-dimensional coordination polymers.

Figure 3. Schematic representation of some basic structural motifs observed for discrete and polymeric metallosupramolecular assemblies containing **dtdp** and mono- or multinuclear metal units as nodes (respectively illustrated by large grey spheres or squares).

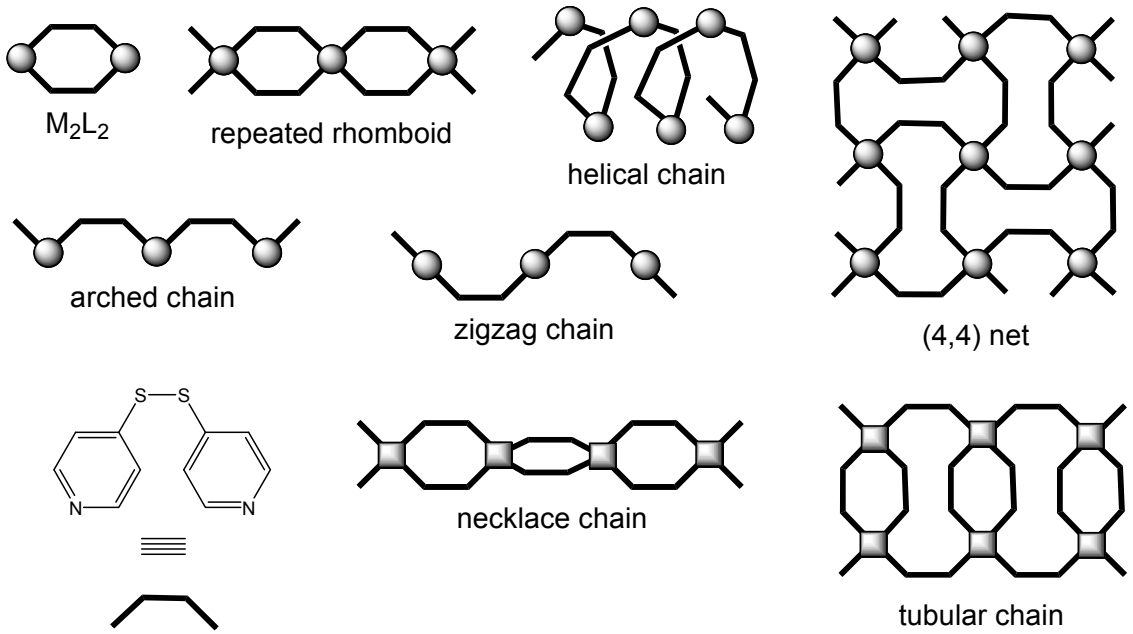

The schematic representation in Figure 3 indicates that coordination polymers of the repeated rhomboid type can be regarded as polymeric strands of M_2L_2 macrocycles fused at the metal corners. This results in an M:L ratio of 1:2. In helical, arched and zigzag chains, the M:L ratio is 1:1 as it is in M_2L_2 macrocycles. If these structures are formed from the same metal units and **dtdp**, they can be viewed as supramolecular isomers [39,40]. There appears to be no strict definition of this term either and hence we think some explanation is necessary. The term supramolecular isomerism was coined by Zaworotko and is chosen to mean the existence of more than one type of supramolecular structure consisting of the same molecular building blocks, in analogy to structural isomerism at the molecular level [39]. Counter-ions and guest molecules that are not directly involved in the formation of the supramolecular structure, for example as ancillary ligands in coordination polymers, do not need to be the same for supramolecular isomers using this definition. This implies that the term supramolecular isomerism is not a synonym for the well-defined term polymorphism, but is somewhat related to the term pseudopolymorphism, which has been coined in the context of molecular crystals [41].

The (4,4) net [42,43] is a common topology in two-dimensional coordination polymers and distorted versions have been obtained from **dtdp** and four-connecting metal nodes. As far as we are able to ascertain, three-dimensional coordination polymers propagated exclusively by **dtdp** as bridging ligands have not been described so far. It appears that the formation of such a structure is less likely owing to the characteristic angular structure of **dtdp** (see Section 1). Necklace and tubular chains represent two examples of topologies found in coordination polymers comprising **dtdp** and multinuclear metal units as nodes. As we shall see, there are also coordination polymers composed of **dtdp** and multinuclear nodes that resemble repeated rhomboid and zigzag chain structures.

3.1. M_2L_2 Macrocycles

Metallamacrocycles composed of two *cis*-configured square-planar or octahedral metal units joined by two **dtdp** ligands (M_2L_2 topology) are achiral or chiral, depending on the conformation of the **dtdp** ligands. The achiral macrocycles contain two **dtdp** ligands of opposite handedness, resulting in a chair-like centrosymmetric structure, whereas the chiral ones exclusively contain two **dtdp** ligands of either the *P* or the *M* form. To our knowledge, only racemic crystals of the latter have been reported so far. Table 1 lists crystallographically characterised M_2L_2 macrocycles containing **dtdp** as bridging ligands.

In general, we need to distinguish between the two main methods of formation of metallo-supramolecular species. The use of more inert *cis*-preconfigured 4d or 5d metal precursors enables self-assembly in solution mainly under thermodynamic control, that is, chemical equilibrium is maintained at all time during the supramolecular reaction. Under appropriate conditions, e.g., solvents, concentration ranges, temperature, solution self-assembly of complementary, geometrically suitable building blocks can give anticipated macrocyclic structures in high yield. This has to be contrasted with non-equilibrium processes. It is generally accepted that crystallisation is mainly a kinetic-based process [44]; the product that forms fastest crystallises first. Crystalline products obtained by the directional-bonding approach using more labile 3d metal precursors assemble at the solvent-crystal interface. In this case, crystallisation can be considered as the supramolecular reaction. It is to be expected, therefore, that kinetic control favours polymerisation rather than the formation of macrocycles. As we shall see, M_2L_2 macrocycles have nevertheless been obtained by crystal engineering with labile 3d metal precursors and **dtdp**. In these cases, the assumption has to be made that packing in the solid-state favours the macrocyclic structure. Since crystal packing is crucially influenced by the nature of co-ligands, counter-ions and solvent molecules, the crystal engineering approach is clearly less straightforward than deliberate synthesis of metallamacrocycles using monodentate bridging ligands by the solution-based directional-bonding approach.

Stang and co-workers were the first to report an M_2L_2 macrocycle with dtdp as bridging ligands in 2001 [45]. When equimolar amounts of *cis*-$[Pt(NO_3)_2(Et_3P)_2]$ and dtdp were allowed to react in methanol-d_4 at room temperature, ^{1}H and ^{31}P-NMR spectroscopy revealed the formation of a closed, symmetric product. The observation of only one set of resonance signals each for the pyridyl groups of **dtdp** and the Et_3P co-ligands is consistent with an M_2L_2 macrocycle with molecular C_{2h} symmetry. Single-crystal X-ray analysis showed the achiral chair-like structure of the macrocycle (XIWNEW), containing a crystallographic centre of symmetry (Figure 4). It is interesting to note that, owing to the inertness of Pt(II) complexes, the *cis*-configuration is retained without a chelate co-ligand. Xiao *et al.*, reported an achiral M_2L_2 macrocycle with Pd(II) corners, *cis*-protected by an *N*-heterocyclic carbene, *viz.* 1,1′-dimesityl-3,3′-methylenediimidazolin-2,2′-diylidene [46]. The macrocycle exhibits crystallographic C_i symmetry, but the molecule adopts approximate C_{2h} point group symmetry (UMUGAL). Achiral macrocycles have also been obtained with half-sandwich complexes, *viz.* $[RuCl(p\text{-cymene})]^+$, as corner units [31]. Both the dichloromethane solvate (GAKHUX) and the chloroform solvate (GAKJAF) of $[\{RuCl(p\text{-cymene})\}_2(\mu\text{-}\mathbf{dtdp})_2](CF_3SO_3)_2$ crystallise with crystallographic inversion symmetry imposed. $[RhCl(Cp^*)]^+$ and $[IrCl(Cp^*)]^+$ (Cp^{*-} = pentamethylcyclopentadienyl) corner units have been used to this end as well, but the metallamacrocycles obtained have not been characterised by X-ray crystallography [31].

Table 1. Selected structural parameters for M_2L_2 macrocycles.

Compound	Molecular Symmetry [a]	C–S–S–C torsion angle (°)	M···M separation (Å)	(S–S)···(S–S) separation (Å)	Reference	CSD Refcode
$[\{Pt(Et_3P)_2\}_2(\mu\text{-dtdp})_2](NO_3)_4\cdot 4CH_3OH$	C_i	91.7	10.96	8.70	[45]	XIWNEW
$[\{Pd(C_{25}H_{28}N_4)\}_2(\mu\text{-dtdp})_2](CF_3SO_3)_4$ [b]	C_{2h}	84.9	10.61	9.06	[46]	UMUGAL
$[\{RuCl(p\text{-cymene})\}_2(\mu\text{-dtdp})_2](CF_3SO_3)_2\cdot 2CH_2Cl_2$	C_i	83.5	10.46	9.53	[31]	GAKHUX
$[\{RuCl(p\text{-cymene})\}_2(\mu\text{-dtdp})_2](CF_3SO_3)_2\cdot 4CHCl_3$	C_i	85.1	10.64	9.36	[31]	GAKJAF
$[\{Ir(H)_2(PPh_3)\}_2(\mu\text{-dtdp})_2](BF_4)_2\cdot 3CH_2Cl_2\cdot H_2O$ [c]	D_2	87.4, 87.2	10.72	9.37	[47]	RUZKIG
$[\{Co(hfacac)_2\}_2(\mu\text{-dtdp})_2]\cdot 4CHCl_3$ [d]	D_2	90.8, 89.2	10.84	9.18	[48]	FEBBEU
$[\{Ni(hfacac)_2\}_2(\mu\text{-dtdp})_2]\cdot 4CHCl_3$ [d]	D_2	91.3, 89.5	10.80	9.13	[48]	FEBBIY
$[\{Co(hfacac)_2\}_2(\mu\text{-dtdp})_2]\cdot H_2O$ [d,e]	C_2	78.5	10.16	9.74	[48]	FEBBOE
$[\{Ni(hfacac)_2\}_2(\mu\text{-dtdp})_2]\cdot H_2O$ [d,e]	C_2	78.0	10.05	9.70	[48]	FEBBUK
$[\{Cu(CF_3SO_3)_2(phen)\}_2(\mu\text{-dtdp})_2]\cdot 0.13H_2O$ [f]	C_i	88.3	10.66	8.98	[28]	INIMOI
$[\{Zn(C_7H_7COO)_2\}_2(\mu\text{-dtdp})_2]$ [g]	C_i	79.6	9.94	9.91	[49]	TAWTIW

[a] The point group symbols refer to the approximate molecular symmetry in the crystal, which is not always identical to the crystallographic site symmetry; [b] Unkown solvate, $C_{25}H_{28}N_4$ = 1,1′-dimesityl-3,3′-methylenediimidazolin-2,2′-diylidene; [c] PPh_3 = triphenylphosphine; [d] $hfacac^-$ = 1,1,1,5,5,5-hexafluoroacetylacetonate; [e] The solvent content is questionable (see text); [f] phen = 1,10-phenanthroline; [g] $C_7H_7COO^-$ = 3-methylbenzoate.

Figure 4. Molecular structure of the achiral M_2L_2 macrocycle in [{Pt(PEt_3)$_2$}$_2$(μ-**dtdp**)$_2$](NO_3)$_4$·4CH_3OH (XIWNEW).

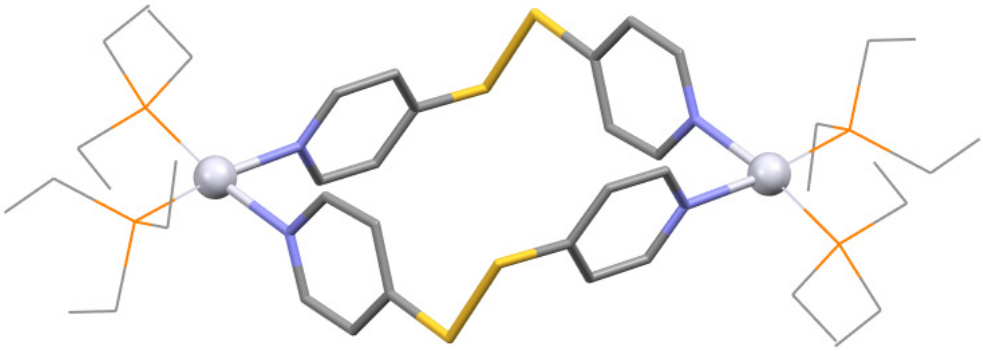

[{Ir(H)$_2$(PPh_3)$_2$}$_2$(μ-**dtdp**)$_2$](BF_4)$_2$ (RUZKIG) represents a chiral macrocycle with approximate molecular D_2 symmetry in the crystal (Figure 5) [47]. RUZKIG was obtained by reaction of [Ir(H)$_2$(PPh_3)$_2$(acetone)$_2$] with **dtdp** in dichloromethane. The Ir(III) ions show a distorted octahedral coordination sphere with the two bulky triphenylphosphine (PPh_3) co-ligands in axial positions. The hydrido co-ligands and **dtdp** bridging ligands each bind to two *cis*-sites in the equatorial plane. In RUZKIG, the configuration of the precursor is also retained despite the absence of chelate co-ligands, which can be explained by the inert nature of Ir(III) complexes.

Figure 5. Molecular structure of the chiral M_2L_2 macrocycle in [{Ir(H)$_2$(PPh_3)$_2$}$_2$(μ-**dtdp**)$_2$](BF_4)$_2$·3CH_2Cl_2·H_2O (RUZKIG). Note that the macrocycle shown contains the left-handed *M* form of **dtdp** in the centrosymmetric crystal structure.

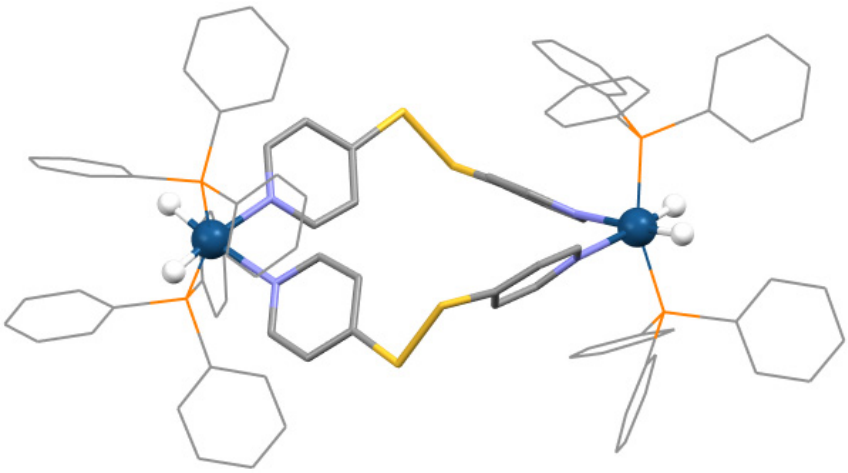

XIWNEW, UMUGAL, GAKHUX, GAKJAF and RUZKIG have also been characterised by NMR spectroscopy, which provides evidence for the existence of the metallamacrocycles in solution. As revealed by the intramolecular M···M and (S–S)···(S–S) distances in the crystal (Table 1), the dimensions of the cavities are clearly too small to accommodate guest molecules. Therefore, it comes as no surprise that molecular recognition features of these metallamacrocycles have not been reported, as far as we can ascertain. The precise shape of the macrocycle, as defined by the C–S–S–C torsion angles and the intramolecular M···M and (S–S)···(S–S) distances (Table 1), is assumed to be affected mainly by the steric demand of the co-ligands at the metal ions and the nature of the

counter-ions and solvent guest molecules, which reside above and below the cavity. In XIWNEW the C–S–S–C torsion angles are the closest to the ideal 90°, which may indicate that the macrocycle is the least strained as compared with UMUGAL, GAKHUX, GAKJAF and RUZKIG. Comparison of the intramolecular M···M and (S–S)···(S–S) distances reveals in turn a more rhomboidally shaped macrocycle in XIWNEW.

M_2L_2 macrocycles derived from **dtdp** and labile 3d metal precursor complexes have been described so far for Co(II), Ni(II), Cu(II) and Zn(II) as metal corners. Horikoshi and co-workers investigated reactions of **dtdp** with $M(hfacac)_2$ (M = Mn^{2+}, Co^{2+}, Ni^{2+} and Cu^{2+}; $hfacac^-$ = 1,1,1,5,5,5-hexafluoroacetylacetonate) complexes [48,50]. Whereas combination of $Mn(hfacac)_2$ and $Cu(hfacac)_2$ units with **dtdp** resulted in zigzag and helical chain coordination polymers (see Section 3.2), M_2L_2 macrocycles were obtained with $Co(hfacac)_2$ and $Ni(hfacac)_2$ corner units [48]. Addition of a solution of $[Co(hfacac)_2(H_2O)_2]$ in diethylether to a solution of an equimolar amount of **dtdp** in chloroform yielded orange crystals of $[\{Co(hfacac)_2\}_2(\mu\text{-}\mathbf{dtdp})_2]\cdot 4CHCl_3$ (FEBBEU). Blue-green crystals of the isostructural $[\{Ni(hfacac)_2\}_2(\mu\text{-}\mathbf{dtdp})_2]\cdot 4CHCl_3$ (FEBBIY) were obtained in analogy by using $[Ni(hfacac)_2(H_2O)_2]$ as precursor complex. Figure 6a shows the molecular structure of FEBBEU in the crystal. Two *cis*-configured $Co(hfacac)_2$ units are joined by two **dtdp** ligands of the same handedness. Furthermore, the presence two chelate co-ligands at each *cis*-$M(hfacac)_2$ corner unit imposes chirality: the left-handed *Λ* form of the *cis*-$Co(hfacac)_2$ and *cis*-$Ni(hfacac)_2$ units are combined with the right-handed *P* form of **dtdp** and *vice versa* in FEBBEU and FEBBIY, respectively. In the crystal, the chiral M_2L_2 macrocycles contain a crystallographic twofold rotation axis, running through the centres of the disulfide moieties. The macrocycles, however, exhibit two additional, approximate non-crystallographic C_2 axis perpendicular to the crystallographic rotation axis. The point group symmetry of the molecule thus resembles D_2.

Mixing a solution of $[Co(hfacac)_2(H_2O)_2]$ and $[Ni(hfacac)_2(H_2O)_2]$ in tetrachloromethane with a solution of **dtdp** in diethylether and recrystallisation of the raw products from diethylether yielded orange and blue-green crystals, reportedly of the composition $[\{Co(hfacac)_2\}_2(\mu\text{-}\mathbf{dtdp})_2]\cdot H_2O$ (FEBBOE) and $[\{Ni(hfacac)_2\}_2(\mu\text{-}\mathbf{dtdp})_2]\cdot H_2O$ (FEBBUK), respectively. FEBBOE and FEBBUK are isostructural like FEBBEU and FEBBIY. Since the crystal structures of FEBBOE und FEBBUK respectively contain solvent accessible voids of *ca.* 309 and 208 $Å^3$ per unit cell volume, the description of the structures as monohydrates must at least be questioned. In contrast to FEBBEU and FEBBIY, the M_2L_2 macrocycles in FEBBOE and FEBBUK comprise two **dtdp** ligands of the same handedness (*i.e.*, either the *P or* the *M* form) and two *cis*-$M(hfacac)_2$ units that are enantiomers (*i.e.*, the left-handed *Λ* and the right-handed Δ form). The molecules thus exhibit C_2 point group symmetry (Figure 6b), which is also the site symmetry in the crystal. The crystallographic twofold rotation axis passes through the two metal atoms in the macrocycle. FEBBOE and FEBBUK may be regarded as supramolecular isomers of FEBBEU and FEBBIY, respectively. For FEBBOE and FEBBUK, the packing of the macrocycles in the crystals is also different from FEBBEU and FEBBIY: not solvent guest molecules but trifluoromethane moieties of adjacent molecules sit above and below the cavity of the macrocycle. It is reasonable to assume that the different stereochemistry of the macrocycles in the chloroform solvates and reported monohydrates is dictated by the crystal packing. Comparison of the structural parameters (Table 1), especially the C–S–S–C torsion angles, indicates that the macrocyclic units in FEBBEO and FEBBUK are significantly more strained than those in FEBBEU and FEBBIY.

Figure 6. (**a**) Molecular structure of the M_2L_2 macrocycle in FEBBEU, showing the *P* form of the **dtdp** ligands and the *Λ* configuration of both *cis*-Co(hfacac)$_2$ corner units; (**b**) Molecular structure of the macrocycle in FEBBOE, also showing the *P* form of the **dtdp** ligands. In this complex, one *cis*-Co(hfacac)$_2$ corner unit adopts the left-handed *Λ* and the other the right-handed Δ configuration (see text).

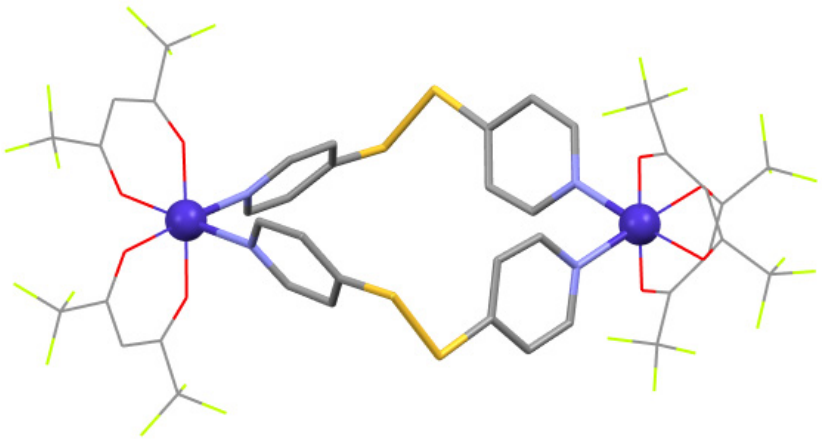

(a)

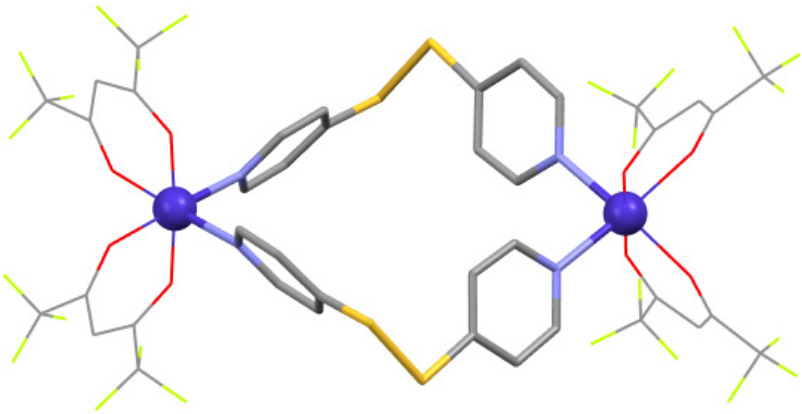

(b)

It has been reported that FEBBEU, FEBBIY, FEBBOE and FEBBUK are soluble in common organic solvents such as chloroform; the macrocyclic complexes are neutral and the hfacac$^-$ co-ligands should enhance the solubility further. Since no solution study (e.g., by optical spectroscopy in the visible region) has been reported, it remains an open question as to whether the equilibrium is on the side of the products, *i.e.*, the macrocycles, and if so, under what conditions, especially concentration ranges. It has furthermore been mentioned that FEBBEU and FEBBIY easily lose the chloroform guest molecules, whereas FEBBOE and FEBBUK are more stable towards loss of solvent guest molecules. Thermogravimetry and powder X-ray diffraction performed on a sample of dried material of FEBBEU indicated that the macrocyclic structure is not retained after removal of the solvent guest molecules. From thermogravimetric analysis of FEBBOE, it has been concluded that the macrocyclic complex is sufficiently stable to sublime [48].

When a pale blue solution of [Cu(CF_3SO_3)$_2$(phen)(H_2O)$_2$] (phen = 1,10-phenanthroline) in aqueous ethanol was layered onto a solution of **dtdp** in dichloromethane, deep blue crystalline material of [{Cu(CF_3SO_3)$_2$(phen)}$_2$(*μ*-**dtdp**)$_2$] (INIMOI) formed spontaneously [28]. The molecular structure in

the crystal represents an M_2L_2 macrocycle, exhibiting a crystallographic inversion centre. Two **dtdp** ligands of opposite handedness join two Cu(II) ions each via two *cis* coordination sites in the equatorial plane of the Jahn-Teller distorted octahedral coordination environment. The remaining two *cis* sites are blocked by the phen chelate co-ligands, and the trifluormethanesulfonate counter-ions are monodentate bound to the apical positions via oxygen atoms of the sulfonate moieties. In the crystal, the macrocycles stack in such a way that $CF_3SO_3^-$ moieties of adjacent molecules are located above and below the cavities. Despite its non-polymeric structure, INIMOI is insoluble in common organic solvents except dimethylsulfoxide. Upon addition of dimethylsulfoxide, a pale blue solution is obtained from INIMOI. Optical spectroscopy in the visible region provided evidence that the metallamacrocyle dissociates into its building blocks under these conditions. *In situ* reaction of cadmium(II) perchlorate, **dtdp** and phen as *cis*-protecting co-ligand resulted in the arched chain coordination polymer $[\{Cd(H_2O)(\mathbf{dtdp})(phen)\}(\mu\text{-}\mathbf{dtdp})(ClO_4)_2{\cdot}2CH_3OH{\cdot}1.5H_2O]_n$ (INIMEY, see Section 3.3).

In situ reaction of **dtdp** with $Zn(NO_3)_2{\cdot}6H_2O$, 3-methylbenzoic acid (C_7H_7COOH) and sodium hydroxide in aqueous methanol afforded colourless crystals of $[\{Zn(C_7H_7COO)_2\}_2(\mu\text{-}\mathbf{dtdp})_2]$ (TAWTIW), which represents another M_2L_2 macrocycle with crystallographically imposed inversion symmetry [49]. Zn(II) ions bearing two bidentate-bound carboxylate groups of 3-methylbenzoate build the corner units; the coordination sphere of Zn(II) is best described as a severely distorted octahedron. The 3-methylbenzoate ligands are *cis* arranged, and owing to the site symmetry in the crystal, the macrocycle necessarily contains both the *Λ* and Δ configuration of the *cis*-$Zn(C_7H_7COO)_2$ corners. TAWTIW contains no solvent guest molecules in the crystal and obviously exhibits an efficient packing of the metallamacrocycles in the crystal, which presumably causes a strained macrocyclic entity, as indicated by the structural parameters in Table 1. It is worth noting that using unsubstituted benzoic acid (C_6H_5COOH) instead of the 3-methyl substituted derivative under similar reaction conditions resulted in the formation of $[Zn(C_6H_5COO)_2(\mu\text{-}\mathbf{dtdp})]_n$ (TAWTES) [49], a coordination polymer with helical chain structure (see Section 3.2). Thus, the presence of a methyl group in the periphery of the co-ligands crucially affects the overall structure of the crystalline product. This clearly indicates that the formation of the metallamacrocyle in TAWTIW is induced by packing effects in the solid-state.

3.2. Repeated Rhomboids

In **dtdp** containing coordination polymers of the repeated rhomboid type, two **dtdp** ligands join two *trans*-configured octahedral metal nodes each via two *cis* coordination sites in the equatorial plane. Repeated rhomboids thus can be viewed as polymeric strands of fused M_2L_2 macrocycles, as mentioned in the previous section. As for discrete M_2L_2 macrocycles, the macrocyclic units can be composed of either two **dtdp** ligands of the same or of the opposite handedness. Likewise, only racemic crystal structures of chiral repeated rhomboids have been observed so far. The polymeric chains of repeated rhomboids are thus either chiral or achiral with chair-like macrocyclic units. The apical positions at the metal ions are occupied by solvent molecules and/or counter-ions. Repeated rhomboids have been reported for Mn(II), Fe(II), Co(II), Cu(II), Zn(II) and Cd(II) so far. Table 2 lists structural parameters of repeated rhomboids, roughly sorted by increasing atomic number of the metal ions involved.

The first coordination polymer with repeated rhomboid structure derived from **dtdp** was reported by Kitagawa and co-workers in 2000 [51]. Slow diffusion of an aqueous solution of $Cd(NO_3)_2{\cdot}4H_2O$ and a solution of **dtdp** in ethanol into one another resulted in colourless crystals of $[\{Cd(H_2O)_2(\mu\text{-}\mathbf{dtdp})_2\}(NO_3)_2{\cdot}2C_2H_5OH{\cdot}2H_2O]_n$ (WOQXUV). The analogous methanol solvate (SOMHOS) has also been described [52]. Both structures represent the achiral type of repeated rhomboids with Cd(II) occupying crystallographic inversion centres. The aqua ligands are in axial positions of the octahedrally coordinated Cd(II) ions. Figure 7a shows the representative structure of a coordination polymer strand in SOMHOS. As revealed by Table 2, a wider variety of repeated rhomboids have been derived from Zn(II) and Cu(II). In 2005, Horikoshi and Mikuriya reported a systematic study of repeated rhomboids obtained from **dtdp** and Zn(II) with various counter-ions and from different solvent systems [53]. In the particular case of zinc(II) nitrate, a variety of structures have been obtained. The solvent-free compound $[Zn(NO_3)_2(\mu\text{-}\mathbf{dtdp})_2]_n$ (FARLUG) represents the chiral type of repeated rhomboids with monodentate nitrato ligands in both apical positions of Zn(II) (Figure 7b). The four pyridyl groups in the equatorial plane adopt a propeller-like arrangement around the metal ion, whereas *trans*-related pyridyl groups are virtually co-planar in achiral repeated rhomboids (Figure 7a). In $[\{Zn(NO_3)(H_2O)(\mu\text{-}\mathbf{dtdp})_2\}NO_3{\cdot}4H_2O]_n$ (FARMAN), one of the nitrato ligands in FARLUG is replaced by an aqua ligand. The nitrato ligand in FARMAN shows rotational disorder about the Zn–O bond at room temperature [53], and a disorder-order-transition upon cooling to 110 K has been observed [54]. In contrast to FARLUG and FARMAN, $[\{Zn(H_2O)_2(\mu\text{-}\mathbf{dtdp})_2\}(NO_3)_2{\cdot}2CH_3OH{\cdot}2H_2O]_n$ (FARLOA) [53] and the corresponding ethanol solvate (PAQMUR) [54] exhibit achiral repeated rhomboids with aqua ligands in apical positions of Zn(II), as in the above-mentioned analogous structures obtained from $Cd(NO_3)_2{\cdot}4H_2O$, SOMHOS and WOQXUV. The methanol solvates, *i.e.*, FARLOA and SOMHOS are isostructural. The metal ions in PAQMUR occupy *pseudo* inversion centres in the already centrosymmetric crystal structure (space group $P\bar{1}$), as opposed to FARLOA, SOMHOS and WOQXUV. $[\{Zn(H_2O)_2(\mu\text{-}\mathbf{dtdp})_2\}(ClO_4)_2{\cdot}2\mathbf{dtdp}]_n$ (FARMIV) and $[\{Zn(dmso)_2(\mu\text{-}\mathbf{dtdp})_2\}(ClO_4)_2]_n$ (FARMER) were obtained by using zinc(II) perchlorate as metal source [53]. In both, the repeated rhomboids are chiral and contain a twofold crystallographic rotation axis, running through the Zn(II) ions along each polymeric strand. FARMIV contains two crystallographically distinct **dtdp** guest molecules of opposite chirality (C–S–S–C torsion angles: 90.3° and −85.9°), which act as acceptors of O–H···N and C–H···N hydrogen bonds. FARLIU and $[Zn(\mu\text{-}SiF_6)(\mu\text{-}\mathbf{dtdp})_2{\cdot}3CH_3OH]_n$ (LEMMAS) represent two further examples of achiral repeated rhomboids with Zn(II) nodes occupying crystallographic inversion centres. BOKXIJ and RAFWAY (Table 2) both exhibit chiral repeated rhomboids, containing crystallographic twofold rotation axes that run along the polymeric strands. BOKXIJ contains hydrogen fumarate as counter-ions, whereas RAFWAY contains the isomeric hydrogen maleate.

Table 2. Selected structural parameters for repeated rhomboids.

Compound	Rhomboids	C–S–S–C torsion angle (°)	M···M separation (Å)	(S–S)···(S–S) separation (Å)	Reference	CSD Refcode
$[Mn(N_3)_2(\mu\text{-dtdp})_2\cdot dtdp]_n$	achiral	87.7, −92.9	11.12	9.28	[55]	DEPVAW
$[Mn(C_6H_5COO)_2(\mu\text{-dtdp})_2\cdot C_6H_5COOH\cdot H_2O]_n$ [a]	chiral	89.3	10.94	9.54	[56]	GEBZAQ
$[Mn(NCS)_2(\mu\text{-dtdp})_2\cdot 0.5dtdp\cdot 0.5H_2O]_n$	achiral	87.6, −87.2 87.1, −86.5	10.89 10.89	9.56 9.58	[57]	–
$[Fe(NCS)_2(\mu\text{-dtdp})_2\cdot 2H_2O]_n$ [b]	chiral	91.2	10.97	9.25	[58]	CEBMAY
$[Fe(NCS)_2(\mu\text{-dtdp})_2\cdot 3H_2O]_n$	chiral	91.8, 91.4	10.93	9.23	[57]	–
$[CoCl_2(\mu\text{-dtdp})_2\cdot 2CH_3OH]_n$	achiral	80.9	10.21	9.59	[58]	CEBMEC
$[Co(NCO)_2(\mu\text{-dtdp})_2\cdot 1.5H_2O]_n$	achiral	82.5 79.1	10.55 10.30	9.69 9.82	[59]	–
$[Co(NCS)_2(\mu\text{-dtdp})_2\cdot dmso]_n$ [c]	chiral	90.0	10.83	9.18	[60]	NIMBIV
$[Co(NCS)_2(\mu\text{-dtdp})_2\cdot 2H_2O]_n$	chiral	91.3	10.91	9.19	[57]	–
$[\{Cu(NO_3)(H_2O)(\mu\text{-dtdp})_2\}NO_3\cdot 3H_2O]_n$	chiral	89.7	10.53	9.15	[61]	EMADIF
$[Cu(\mu\text{-}SO_4)(\mu\text{-dtdp})_2\cdot 2CH_3OH\cdot 3H_2O]_n$	chiral	88.4	10.55	9.12	[61]	EMADEB
$[\{Cu(\mu\text{-}N_3)(\mu\text{-dtdp})_2\}ClO_4\cdot 5H_2O]_n$	chiral	92.2	10.84	8.89	[62]	GANPER
$[Cu(ClO_4)_2(\mu\text{-dtdp})_2\cdot 3H_2O]_n$	chiral	91.7	10.70	8.89	[63]	VILKUX
$[\{Cu(H_2O)_2(\mu\text{-dtdp})_2\}(C_5H_4NSO_3)_2\cdot 2H_2O]_n$ [d]	chiral	89.0	10.70	9.04	[64]	VUKGAK
$[Cu(C_5H_4NSO_3)_2(\mu\text{-dtdp})_2\cdot 2H_2O]_n$ [d]	chiral	88.7	10.56	9.06	[64]	VUKGEO
$[\{Cu(H_2O)_2(\mu\text{-dtdp})_2\}(C_8H_5O_4)_2\cdot H_2O]_n$ [e]	chiral	90.5, 89.1	10.73	8.96	[65]	DUMBAP
$[\{Cu(H_2O)_2(\mu\text{-dtdp})_2\}(CF_3SO_3)_2]_n$	chiral	84.8, 82.6	10.36	9.33	[66]	UJEXAJ
$[\{Cu(H_2O)_2(\mu\text{-dtdp})_2\}(C_4H_3O_4)_2\cdot 4H_2O]_n$ [f]	chiral	92.2	10.77	8.87	[67]	RAFVUR
$[\{Cu(H_2O)_2(\mu\text{-dtdp})_2\}(C_5H_4NSO_3)_2]_n$ [g]	chiral	89.3	10.72	8.97	[67]	RAFVIF
$[Zn(NO_3)_2(\mu\text{-dtdp})_2]_n$	chiral	87.3, 87.1	10.88	9.23	[53]	FARLUG
$[\{Zn(NO_3)(H_2O)(\mu\text{-dtdp})_2\}NO_3\cdot 4H_2O]_n$	chiral	88.9, 88.9	10.67	9.37	[53,54]	FARMAN
$[\{Zn(H_2O)_2(\mu\text{-dtdp})_2\}(NO_3)_2\cdot 2CH_3OH\cdot 2H_2O]_n$	achiral	91.1	10.89	9.19	[53]	FARLOA
$[\{Zn(H_2O)_2(\mu\text{-dtdp})_2\}(NO_3)_2\cdot 2C_2H_5OH\cdot 2H_2O]_n$	achiral	93.8, −93.2	11.02	9.09	[54]	PAQMUR
$[\{Zn(H_2O)_2(\mu\text{-dtdp})_2\}(ClO_4)_2\cdot 4dtdp]_n$	chiral	90.2	10.86	9.25	[53]	FARMIV

Table 2. *Cont.*

Compound	Rhomboids	C–S–S–C torsion angle (°)	M···M separation (Å)	(S–S)···(S–S) separation (Å)	Reference	CSD Refcode
$[\{Zn(dmso)_2(\mu\text{-dtdp})_2\}(ClO_4)_2]_n$ [c]	chiral	88.8	10.82	9.27	[53]	FARMER
$[Zn(NCS)_2(\mu\text{-dtdp})_2\cdot 2dmf]_n$ [h]	achiral	86.0	10.61	9.59	[53]	FARLIU
$[Zn(\mu\text{-}SiF_6)(\mu\text{-dtdp})_2\cdot 3CH_3OH]_n$	achiral	85.4	10.62	9.47	[68]	LEMMAS
$[\{Zn(H_2O)_2(\mu\text{-dtdp})_2\}(C_4H_3O_4)_2]_n$ [f]	chiral	92.5	11.09	8.83	[69]	BOKXIJ
$[Zn(C_7H_7COO)_2(\mu\text{-dtdp})_2\cdot H_2O]_n$ [i]	chiral	97.1, 93.4	11.19	8.80	[70]	QUXMUS
$[\{Zn(H_2O)_2(\mu\text{-dtdp})_2\}(C_4H_3O_4)_2\cdot 5H_2O]_n$ [j]	chiral	91.5	10.95	9.18	[67]	RAFWAY
$[\{Zn(H_2O)_2(\mu\text{-dtdp})_2\}(C_5H_4NSO_3)_2\cdot 2H_2O]_n$ [g]	chiral	89.3	10.80	9.19	[67]	RAFVOL
$[\{Cd(H_2O)_2(\mu\text{-dtdp})_2\}(NO_3)_2\cdot 2CH_3OH\cdot 2H_2O]_n$	achiral	88.8	11.01	9.48	[52]	SOMHOS
$[\{Cd(H_2O)_2(\mu\text{-dtdp})_2\}(NO_3)_2\cdot 2C_2H_5OH\cdot 2H_2O]_n$	achiral	89.7	11.11	9.50	[51]	WOQXUV

[a] $C_6H_5COO^-$ = benzoate; [b] The structure has been reported as a tetrahydrate, but a close inspection of the crystal structure revealed that the description as a dihydrate is more appropriate; [c] dmso = dimethylsulfoxide; [d] $C_5H_4NSO_3^-$ = pyridine-4-sulfonate; [e] $C_8H_5O_4^-$ = hydrogen phthalate; [f] $C_4H_3O_4^-$ = hydrogen maleate; [g] $C_5H_4NSO_3^-$ = pyridine-3-sulfonate; [h] dmf = *N*,*N*-dimethylformamide; [i] $C_7H_7COO^-$ = phenyl acetate; [j] $C_4H_3O_4^-$ = hydrogen fumarate.

For Cu(II), an almost equal number of repeated rhomboids as for Zn(II) have been reported (Table 2). Interestingly, only chiral repeated rhomboids derived from Cu(II) have been described so far. The majority, that is EMADEB, GANPER, VILKUX, VUKGAK, VUKGEO, RAFVIF and RAFVUR contain twofold rotation axes running along the polymeric strands in the crystal. EMADIF contains crystallographic twofold rotation axes passing through the Cu(II) ions perpendicular to the direction of propagation of the repeated rhomboids, whereas each two crystallographically unique **dtdp** ligands of the same chirality form the rhomboids in DUMBAP and $[\{Cu(H_2O)_2(\mu\text{-}\mathbf{dtdp})_2\}(CF_3SO_3)_2]_n$ (UJEXAJ) [65,66]. $[\{Cu(H_2O)_2(\mu\text{-}\mathbf{dtdp})_2\}(C_5H_4NSO_3)_2{\cdot}2H_2O]_n$ (VUKGAK) contains pyridine-4-sulfonate ($C_5H_4NSO_3^-$), resulting from partial *in situ* oxidative cleavage of **dtdp**, as counter-ions and $[\{Cu(H_2O)_2(\mu\text{-}\mathbf{dtdp})_2\}(C_5H_4NSO_3)_2]_n$ (VUKGEO) as ancillary ligands. Carballo *et al.*, reasoned that the cleavage of **dtdp**, which occurred under ambient conditions in mixtures containing Cu(II) formate or acetate, was mediated by Cu(II) [64]. It is worthy of note that in VUKGEO the pyridine-4-thiolate binds to the apical positions of Cu(II) via a sulfonate oxygen atom, which is considered a weaker ligand than the pyridyl group. This is characteristic of octahedral Cu(II) complexes and has been attributed to a more electrostatic interaction between Cu(II) and the axial ligands as a result of the Jahn-Teller effect, associated with the d^9 electronic configuration [71]. Temperature-dependent measurements of the magnetic susceptibility of EMADIF and VILKUX revealed weak antiferromagnetic coupling of the Cu(II) ions [61,63], consistent with the *intra*chain M···M separations (Table 2). In EMADEB and GANPER, however, the strands of repeated rhomboids are further connected by the axial μ-sulfato and μ-azido ancillary ligands, respectively. *Inter*chain ferromagnetic interactions were observed for the μ-sulfato-linked EMADEB [61], whereas weak antiferromagnetic coupling through the μ-azido bridges was reported for GANPER [62].

Figure 7. (**a**) Achiral repeated rhomboid strand in $[\{Cd(H_2O)_2(\mu\text{-}\mathbf{dtdp})_2\}(NO_3)_2{\cdot}2CH_3OH{\cdot}2H_2O]_n$ (SOMHOS); (**b**) Chiral repeated rhomboid strand in $[Zn(NO_3)_2(\mu\text{-}\mathbf{dtdp})_2]_n$ (FARLUG). Note that the polymer strand shown contains the right-handed *P* form of **dtdp** in the centrosymmetric crystal structure.

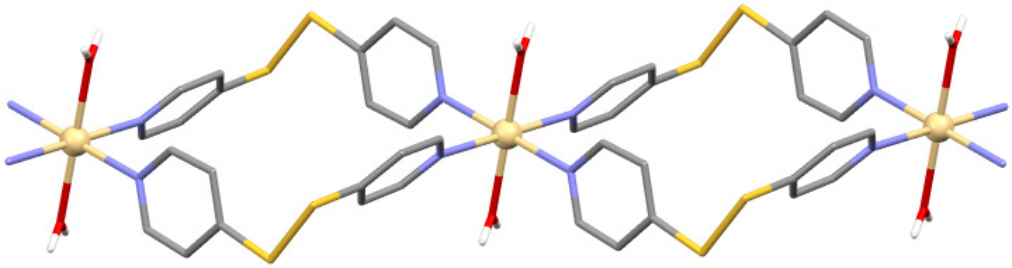

(a)

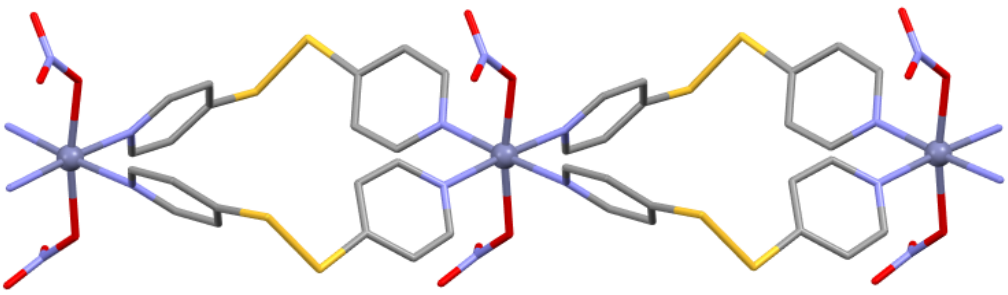

(b)

Repeated rhomboids derived from transition metal ions other than Cu(II) are scarce. In 2005, Suen *et al*. reported $[Fe(NCS)_2(\mu\text{-}\mathbf{dtdp})_2\cdot 2H_2O]_n$ (CEBMAY) and $[CoCl_2(\mu\text{-}\mathbf{dtdp})_2\cdot 2CH_3OH]_n$ (CEBMEC), exhibiting chiral and achiral rhomboids, respectively [58]. CEBMEC is the sole example of repeated rhomboids containing halide ions, and interestingly the axial Co–Cl distances of 2.92 Å are considerably longer than those of 2.44 Å in *trans*-$[CoCl_2(pyridine)_4]$ (TPYRCO01) [72] with a propeller-like arrangement of the four pyridine ligands. The Jahn-Teller distortion characteristic of a d^7 low-spin electronic configuration of Co(II) could provide a plausible explanation for the increased axial Co–Cl bond lengths in CEBMEC. Magnetic properties, however, were reported neither for CEBMEC nor for NIMBIV, the latter of which exhibits chiral rhomboids with isothiocyanato ancillary ligands at the apical positions of Co(II) [60]. In 2012, Cortés and co-workers reported structures and properties of $[Mn(NCS)_2(\mu\text{-}\mathbf{dtdp})_2\cdot 0.5\mathbf{dtdp}\cdot 0.5H_2O]_n$, $[Fe(NCS)_2(\mu\text{-}\mathbf{dtdp})_2\cdot 3H_2O]_n$ and $[Co(NCS)_2(\mu\text{-}\mathbf{dtdp})_2\cdot 2H_2O]_n$ [57]. The coordination network in $[Fe(NCS)_2(\mu\text{-}\mathbf{dtdp})_2\cdot 3H_2O]_n$ is isostructural to that in CEBMAY. For $[Fe(NCS)_2(\mu\text{-}\mathbf{dtdp})_2\cdot 3H_2O]_n$, *Cc* space group symmetry with a β angle of the monoclinic unit cell close to 90° [91.97(1)°] and twinning by a twofold rotation about the c^* direction was reported, whereas CEBMAY was described in the orthorhombic space group *Ccc*2 [58], which is a supergroup of *Cc*. The remarkable similarity between the two structures raises questions about the role of the water molecules in the crystal packing. $[Co(NCS)_2(\mu\text{-}\mathbf{dtdp})_2\cdot 2H_2O]_n$ and CEBMAY are in contrast isomorphous. Temperature-dependent magnetic susceptibility measurements indicated slight antiferromagnetic coupling in $[Fe(NCS)_2(\mu\text{-}\mathbf{dtdp})_2\cdot 3H_2O]_n$ and $[Co(NCS)_2(\mu\text{-}\mathbf{dtdp})_2\cdot 2H_2O]_n$. Very recently, again the group of Cortés reported on the structure and properties of $[Co(NCO)_2(\mu\text{-}\mathbf{dtdp})_2\cdot 1.5H_2O]_n$ [59]. The compound features two crystallographically distinct strands of achiral repeated rhomboids, which cross in the crystal, one strand extending in the [100] and the other in the [010] direction of the triclinic unit cell. Temperature-dependent magnetic susceptibility measurements performed at different fields indicated a spin canting phenomenon.

Interestingly, two structures derived from Mn(II), namely $[Mn(N_3)_2(\mu\text{-}\mathbf{dtdp})_2\cdot\mathbf{dtdp}]_n$ (DEPVAW) [55] and $[Mn(NCS)_2(\mu\text{-}\mathbf{dtdp})_2\cdot 0.5\mathbf{dtdp}\cdot 0.5H_2O]_n$ [57], are the only examples of repeated rhomboids that crystallise in a Sohncke space group ($P2_1$), *i.e.*, a space group that contains no mirror planes, glide planes or inversion centres. In both structures, the rhomboids are, however, formed from two crystallographically distinct **dtdp** ligands of opposite chirality and therefore the coordination polymers are labelled achiral in Table 2. Although there are significant differences in the C–S–S–C torsion angles, the *P* and *M* forms of **dtdp** are approximately related by *local* inversion centres within the repeated rhomboids, which do not extend to the rest of the structure. The asymmetric unit of DEPVAW contains a guest **dtdp** molecule in *M* conformation (C–S–S–C torsion angle: −91.5°), but it should be noted that the crystal studied was a twin by inversion, as indicated by a Flack x parameter of 0.33(2) [73], so both hands were present in the crystal studied. $[Mn(NCS)_2(\mu\text{-}\mathbf{dtdp})_2\cdot 0.5\mathbf{dtdp}\cdot 0.5H_2O]_n$ contains two crystallographically distinct achiral strands of repeated rhomboids. The asymmetric unit furthermore contains a disordered **dtdp** guest molecule, which has been described with a split model comprising the *P* and *M* forms. According to the Flack x parameter of 0.02(2), the crystal studied was enantiopure, but it has not been reported whether the bulk sample was enantiopure or a conglomerate. Considering that the starting material was racemic, the latter seems more likely. $[Mn(C_6H_5COO)_2(\mu\text{-}\mathbf{dtdp})_2\cdot C_6H_5COOH\cdot H_2O]_n$ (GEBZAQ), a chiral repeated rhomboid coordination polymer from Mn(II) with benzoato ancillary ligands, was reported recently [56]. From temperature-dependent

magnetic susceptibility measurements of DEPVAW, $[Mn(NCS)_2(\mu\text{-}\mathbf{dtdp})_2\cdot 0.5\mathbf{dtdp}\cdot 0.5H_2O]_n$ and GEBZAQ, the authors of the studies concluded that the Mn(II) ions are in high-spin state with respectively very weak antiferromagnetic coupling [55,57] and no significant magnetic interaction [56], as expected in view of the long intrachain M···M distances (Table 2).

The listing in Table 2 reveals that chiral repeated rhomboids represent the majority of the structures that have been reported so far. Nevertheless, no simple correlation between the conformational preference of **dtdp** and the nature of the metal nodes, ancillary ligands, counter-ions and guest molecules is obvious. It is interesting to note that the cationic coordination polymer $[Zn(H_2O)_2(\mu\text{-}\mathbf{dtdp})_2]_n^{n2+}$ exhibits achiral rhomboids in FARLOA and PAQMUR but chiral ones in BOKXIJ. This phenomenon can be described as conformational supramolecular isomerism [39]. In most cases, a compact arrangement of adjacent repeated rhomboid strands that are parallel in the crystal is achieved as shown Figure 8a, resulting in corrugated layers (Figure 8b). These are offset or face-to-face stacked in the third dimension (Figure 9). Face-to-face stacking results in a pillared structure. As with discrete M_2L_2 macrocycles (see Section 3.1), counter-ions, guest molecules or ancillary ligands of an adjacent strand reside above and below the cavities of the rhomboids. Guest molecules with hydrogen bonding donor capabilities, such as methanol, ethanol and water, are mostly involved in intricate hydrogen bonding networks in the crystal. The packing of the repeated rhomboid strands in DEPVAW and UJEXAJ resembles a herring-bone pattern. With a tetragonal crystal structure (space group $P\bar{4}$), the arrangement of the repeated rhomboid strands in FARMER is also remarkably different from the other examples. As aforementioned, in EMADEB and GANPER the strands that are face-to-face stacked are joined into two-dimensional coordination networks via the axial coordination sites of Cu(II) through μ-sulfato and μ-azido ancillary ligands, respectively. LEMMAS is a unique example of repeated rhomboids linked into a three-dimensional coordination network [68]. In the crystal, the strands that are crossed, extending in the [110] and [1 $\bar{1}$ 0] directions, are connected through μ-hexafluorosilicato ancillary ligands via the apical positions of Zn(II) in the [001] direction. It is intriguing that in all the crystal structures described in this section, the metal atoms in the individual repeated rhomboid strands ···M···M···M···M··· are despite different crystal environments colinear, although they need not be.

Figure 8. (**a**) Compact arrangement of two adjacent repeated rhomboid strands and (**b**) corrugated layers viewed along the direction of propagation of the strands in $[\{Cd(H_2O)_2(\mu\text{-}\mathbf{dtdp})_2\}(NO_3)_2\cdot 2CH_3OH\cdot 2H_2O]_n$ (SOMHOS) with nitrate ions and solvent molecules sandwiched in between.

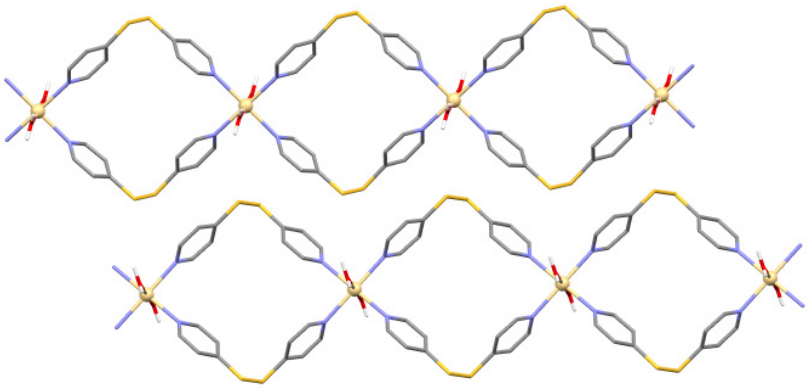

(a)

Figure 8. *Cont.*

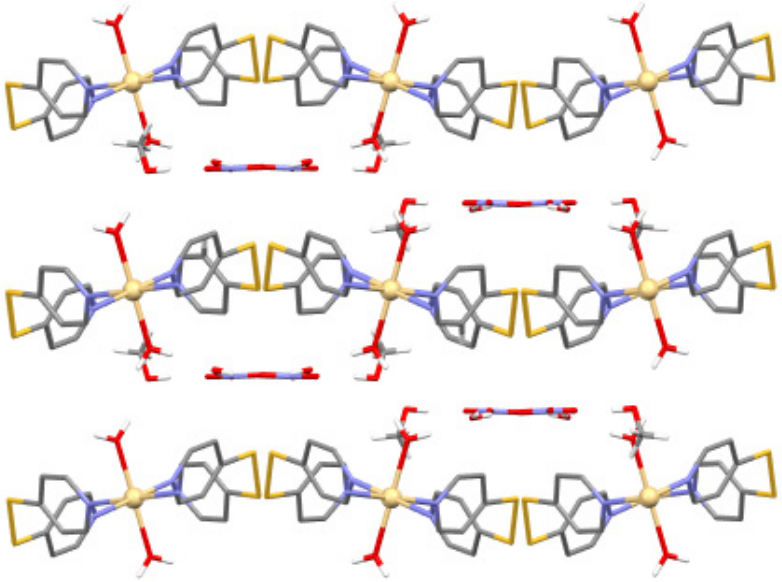

(b)

Figure 9. (**a**) Off-set stacking of two adjacent strands in $[Zn(NO_3)_2(\mu\text{-}\mathbf{dtdp})_2]_n$ (FARLUG) and (**b**) face-to-face stacking in $[\{Cu(H_2O)_2(\mu\text{-}\mathbf{dtdp})_2\}(C_4H_3O_4)_2{\cdot}4H_2O]_n$ (RAVFUR).

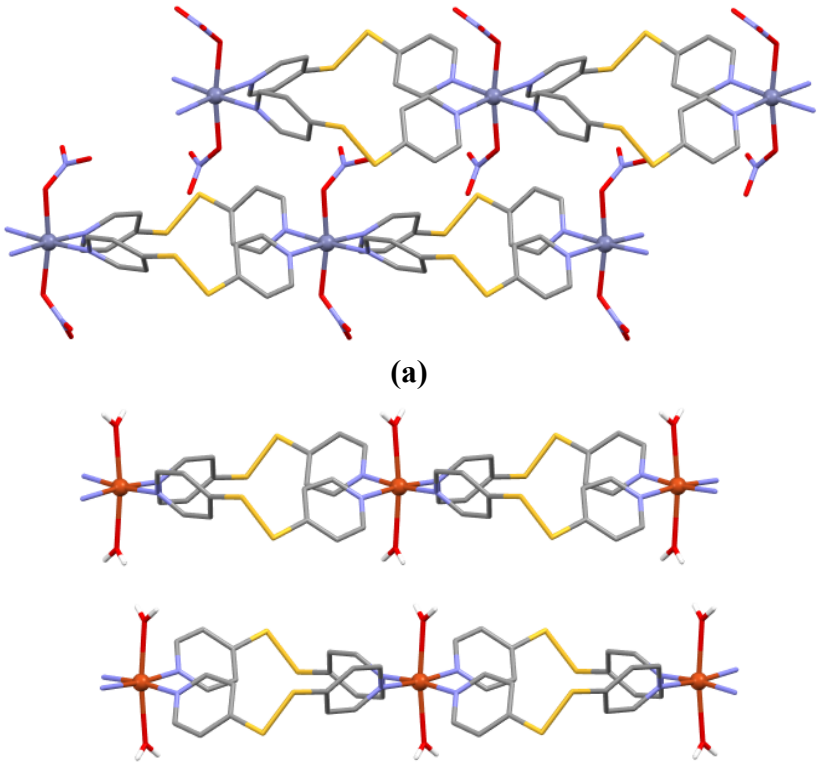

(a)

(b)

3.3. Arched Chains

Table 3 lists coordination polymers of the arched chain type derived from **dtdp**. These consist of angular metal fragments linked by just one **dtdp** moiety to form open polymeric chains. The metal nodes are mostly provided by tetrahedrally or *cis*-configured octahedrally coordinated metal ions.

The structures in Table 3 are sorted by increasing atomic number of the metal ions serving as nodes. In all structures, the arched chains exclusively contain one enantiomer of **dtdp**, although neighbouring chains contain perforce the other enantiomer, since the crystal structures are without exception centrosymmetric and thus racemic. $[Cd(C_6H_{14}O_2PS_2)_2(\mu\text{-}\mathbf{dtdp})]_n$ (BILFAE), the first example of an arched chain with **dtdp** bridges, was reported by Lai and Tiekink in 2004 [74]. The corresponding Zn(II) derivative exhibits a distorted zigzag chain structure (see Section 3.4 and Figure 3). Figure 10a depicts an arched chain strand in BILFAE, composed of *cis*-$[Cd(C_6H_{14}O_2PS_2)_2]$ ($C_6H_{14}O_2S_2^-$ = *O*,*O*′-diisopropyldithiophosphate) fragments joined by **dtdp** via the two remaining *cis* sites of Cd(II). The configuration of the *cis*-$[Cd(C_6H_{14}O_2PS_2)_2]$ units and the conformation of **dtdp** exhibit the same handedness in one arched chain. Thus, in one polymer strand the *P* form of **dtdp** links *cis* metal units in Δ configuration, whereas in symmetry-related strands the *M* form of **dtdp** joins *cis* metal units in *Λ* configuration. The C–S–S–C torsion angle in BILFAE at 74.3° is remarkably smaller than the ideal 90°. The same holds for $N_{pyridine}$–Cd–$N_{pyridine}$ bond angle of 81.2°. The intrachain M···M distance is the shortest observed in arched chains. Additionally, there is a calculated void of 16.84 Å^3 at the origin of the unit cell. These structural parameters indicate that the arched chains in BILFAE are the most compressed in the direction of propagation in the crystal of the arched chain structures listed in Table 3. This contrasts strongly with $[Co(H_2O)_2(C_5O_5)(\mu\text{-}\mathbf{dtdp})\cdot 1.5H_2O]_n$ ($C_5O_5^{2-}$ = croconate) (TEZQUL) [75], in which torsion angles of 91.7° and 101.7° are observed. It is interesting to note that the asymmetric units of TEZQUL and $[\{Cd(H_2O)(\mathbf{dtdp})(phen)\}(\mu\text{-}\mathbf{dtdp})(ClO_4)_2\cdot 2CH_3OH\cdot 1.5H_2O]_n$ (INIMEY) [28] in the crystal each contain two chemically similar but crystallographically distinct ML repeat units of the coordination polymers, which can be interpreted in terms of $Z' = 2$ [76,77], and these independent units are alternately incorporated in the respective chains with the same chirality. The polymer strands are interlaced in TEZQUL and parallel to one another in INIMEY. As shown in Table 3, the C–S–S–C torsion angles corresponding to the *μ*-**dtdp** ligands are virtually equal in INIMEY but differ greatly in TEZQUL. In contrast to BILFAE, the right-handed *P* form of **dtdp** and *cis*-$[Co(H_2O)_2(C_5O_5)]$ exhibiting the left-handed *Λ* configuration in TEZQUL form an arched chain and *vice versa* (Figure 10b).

Table 3. Selected structural parameters for arched chains.

Compound	C–S–S–C torsion angle (°)	M···M separation (Å)	Reference	CSD Refcode
$[Co(H_2O)_2(C_5O_5)(\mu\text{-dtdp})\cdot 1.5H_2O]_n$ [a]	91.7, 101.7	11.00, 12.40	[75]	TEZQUL
$[Cu(C_2H_3O_3)_2(\mu\text{-dtdp})\cdot 4H_2O]_n$ [b]	82.9	10.17	[26]	UFAVED
$[Cu(C_3H_5O_3)_2(\mu\text{-dtdp})\cdot 4H_2O]_n$ [c]	88.9	10.51	[78]	TOKDUT
$[\{Cu(NO_3)(H_2O)(en)(\mu\text{-dtdp})\}NO_3\cdot 4H_2O]_n$ [d]	98.4	11.09	[79]	FOTVEQ
$[Zn(CH_3COO)_2(\mu\text{-dtdp})]_n$	89.6	10.94	[80,81]	FAYQUS
$[Zn(NCS)_2(\mu\text{-dtdp})]_n$	91.5	11.05	[58,81]	CEBLUR
$[ZnCl_2(\mu\text{-dtdp})]_n$	91.8	10.95	[82]	YEJDAU
$[ZnBr_2(\mu\text{-dtdp})]_n$	89.9	10.84	[83]	–
$[Zn(C_6H_5COO)_2(\mu\text{-dtdp})]_n$ [e]	93.9	11.15	[49]	TAWTES
$[Cd(C_6H_{14}O_2PS_2)_2(\mu\text{-dtdp})]_n$ [f]	74.3	9.88	[74]	BILFAE
$[\{Cd(H_2O)(dtdp)(phen)\}(\mu\text{-dtdp})(ClO_4)_2\cdot 2CH_3OH\cdot 1.5H_2O]_n$	86.2, 86.0 85.3 [g], 90.7 [g]	10.70, 10.84	[28]	INIMEY

[a] $C_5O_5^{2-}$ = croconate; [b] $C_2H_3O_3^-$ = glycolate; [c] $C_3H_5O_3^-$ = lactate; [d] en = ethylenediamine; [e] $C_6H_5COO^-$ = benzoate; [f] $C_6H_{14}O_2PS_2^-$ = *O*,*O*′-diisopropyldithiophosphate; [g] Refers to the terminal **dtdp** ligands.

Figure 10. (**a**) Arched chain in $[Cd(C_6H_{14}O_2S_2)_2(\mu\text{-}\mathbf{dtdp})]_n$ (BILFAE), showing the right-handed *P* form of **dtdp** and the right-handed Δ configuration of the *cis*-octahedral metal units; (**b**) Arched chain in $[Co(H_2O)_2(C_5O_5)(\mu\text{-}\mathbf{dtdp})\cdot 1.5H_2O]_n$ (TEZQUL), showing the *P* form of the crystallographically distinct **dtdp** ligands and the left-handed *Λ* configuration of the metal units.

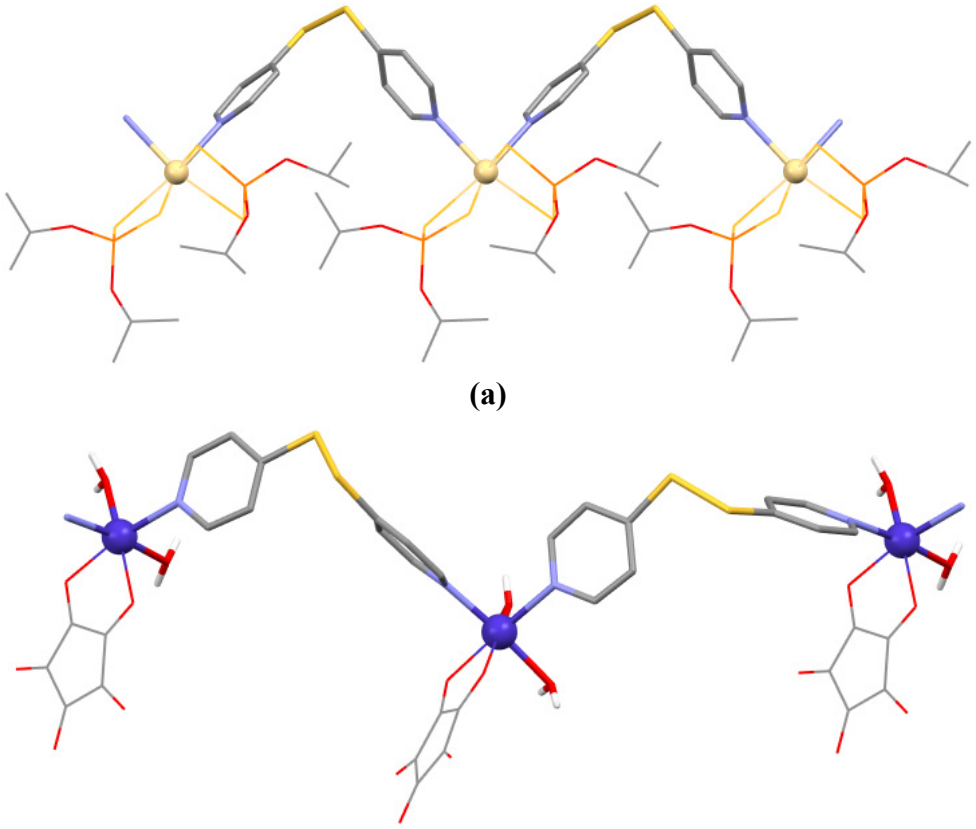

(a)

(b)

As far as we are able to ascertain, INIMEY is the sole example of a structure in which *μ*-bridging and terminal **dtdp** ligands coexist (Figure 11), whereas 4,4′-bipyridine has been frequently observed coexisting as *μ*-bridging and terminal ligands in coordination polymers [84,85]. The scarcity of similar structures derived from **dtdp** has been addressed in the introduction. Interestingly, the two terminal **dtdp** ligands in the asymmetric unit of INIMEY are of the same handedness (C–S–S–C torsion angles: 90.7° and 85.3°) as the two *μ*-bridging ones. The non-coordinating pyridyl groups act as acceptors for O–H···N hydrogen bonds. The phen co-ligands at the metal were purposefully introduced as *cis*-protecting groups, and it is worth pointing out that a polymeric arched chain resulted from self-assembly with **dtdp** rather than an M_2L_2 macrocycle like in INIMOI, which was obtained from $[Cu(CF_3SO_3)(phen)(H_2O)_2]$ as *cis*-preconfigured metal precursor (see Section 3.1).

Figure 11. Arched chain in [{Cd(H_2O)(**dtdp**)(phen)}(μ-**dtdp**)(ClO_4)$_2$·2CH_3OH·1.5H_2O]$_n$ (INIMEY), showing both crystallographically distinct μ-**dtdp** ligands (all **dtdp** ligands shown exhibit the *P* conformation).

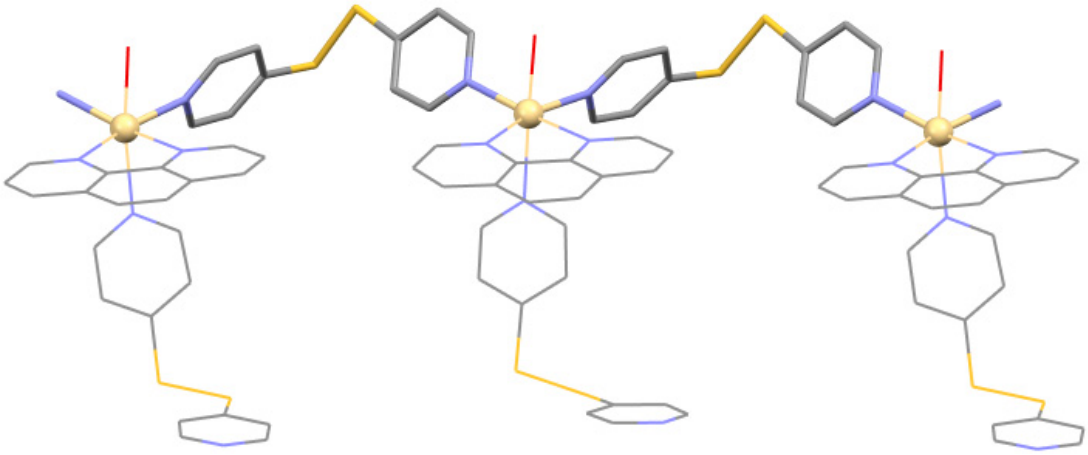

In situ reaction of Cu(NO_3)$_2$·3H_2O, ethylenediamine (en) and **dtdp** yielded dark blue crystals of [{Cu(NO_3)(H_2O)(en)(μ-**dtdp**)}NO_3·4H_2O]$_n$ (FOTVEQ) [79]. As anticipated, the en chelate ligand acts as *cis*-protecting co-ligand in the equatorial plane of the coordination sphere of Cu(II). The *cis* metal units so formed are joined by **dtdp** via the two remaining equatorial *cis* coordination sites to form an arched chain (Figure 12). The octahedral coordination sphere of Cu(II) is completed by an aqua and a nitrato ligand in the two apical positions. Owing to the twisted conformation, five-membered chelate rings formed from en are chiral. In FOTVEQ, the right-handed *P* form of **dtdp** forms a polymer strand with the left-handed λ form of the Cu(en)$^{2+}$ entities and *vice versa*.

Figure 12. Arched chain in [{Cu(NO_3)(H_2O)(en)(μ-**dtdp**)}NO_3·4H_2O]$_n$ (FOTVEQ), showing the right-handed *P* form of **dtdp** and the left-handed λ form of the Cu(en)$^{2+}$ units.

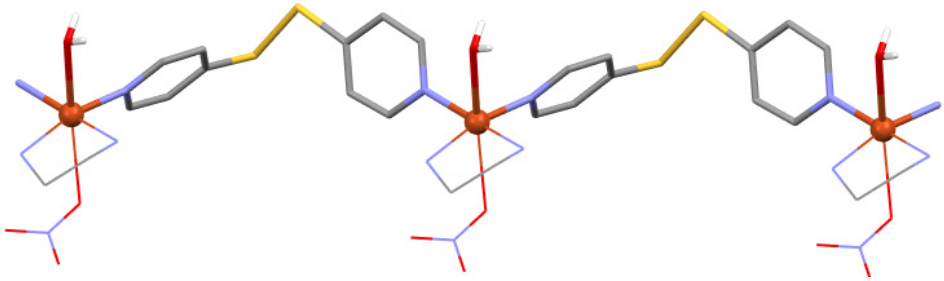

Carballo *et al.* reported two arched chains that are essentially similar to BILFAE. In [Cu(glycolate)$_2$(μ-**dtdp**)·4H_2O]$_n$ (UFAVED) [26] and [Cu(lactate)$_2$(μ-**dtdp**)·4H_2O]$_n$ (TOKDUT) [78], the **dtdp** linkages and the *cis*-Cu(glycolate)$_2$ and *cis*-Cu(lactate)$_2$ units, respectively, exhibit the same chirality in each polymer strand. Interestingly, the configuration of the lactato co-ligands in TOKDUT is also of the same handedness (Figure 13). In UFAVED, twofold crystallographic rotation axes run through the centre of the disulfide moiety and the metal corner unit perpendicular to the direction of propagation of the polymer strands.

Figure 13. Arched chain in $[Cu(lactate)_2(\mu\text{-}\mathbf{dtdp})\cdot 4H_2O]_n$ (TOKDUT), showing the *P* form of **dtdp** and Δ-configured *cis*-Cu(*R*-lactate)$_2$ units.

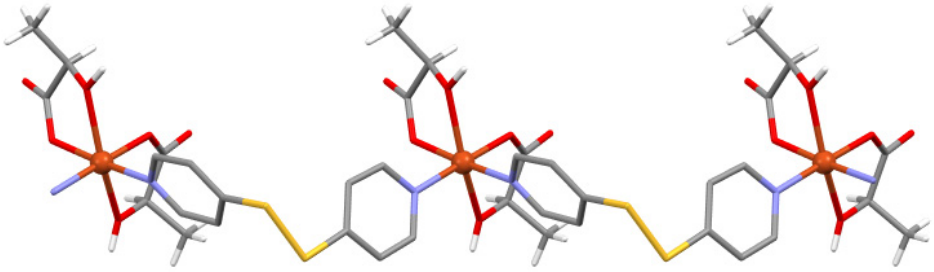

$[Zn(CH_3COO)_2(\mu\text{-}\mathbf{dtdp})]_n$ (FAYQUS) [80,81], $[Zn(NCS)_2(\mu\text{-}\mathbf{dtdp})]_n$ (CEBLUR) [58,81], $[ZnCl_2(\mu\text{-}\mathbf{dtdp})]_n$ (YEJDAU) [82] and $[ZnBr_2(\mu\text{-}\mathbf{dtdp})]_n$ [83] form an isomorphous series of arched chains, in which tetrahedrally coordinated Zn(II) ions are joined by **dtdp**. In each case, two monodentate-bound acetato (FAYQUS01), isothiocyanato (CEBLUR01) and chlorido (CEBLUR01) ancillary ligands complete the coordination sphere of Zn(II). In the crystal, arched chains formed from μ-**dtdp** ligands of opposite chirality are tightly packed, as shown for CEBLUR01 in Figure 14. All three structures crystallise with *C*2/*c* space group symmetry with the twofold crystallographic rotation axes in the [010] direction passing through the centre of the disulfide moieties of **dtdp** and the Zn(II) ions. In YEJDAU, the chlorido derivative, the β angle of the monoclinic unit cell is close to 90° with a value of 92.37(2)° and the crystal studied was a non-merohedral twin. The twin operation is a twofold rotation about the [001] direction, which coincides with the direction of propagation of the polymer strands in the crystal. The same sort of twinning was found in the bromido analogue, $[ZnBr_2(\mu\text{-}\mathbf{dtdp})]_n$ [β = 91.21(3)°]. In $[Zn(C_6H_5COO)_2(\mu\text{-}\mathbf{dtdp})]_n$ (TAWTES), the arrangement of the arched chains with benzoato ancillary ligands in the coordination sphere of Zn(II) is essentially comparable [49]. The Zn–$O_{carboxylate}$ distances for the two benzoato ligands are 1.95/2.54 and 1.95/2.96 Å. Thus, the coordination modes may be regarded as asymmetric bidentate and monodentate, respectively. Accordingly, the coordination environment of Zn(II) can be described as a severely distorted trigonal-bipyramid. As mentioned in Section 3.1, introducing 3-methylbenzoato co-ligands under similar conditions yielded an M_2L_2 macrocycle (TAWTIW), which reveals a structure-determining influence of the methyl group in the periphery of the benzoato co-ligands.

Figure 14. Compact arrangement of two adjacent arched chains in $[Zn(NCS)_2(\mu\text{-}\mathbf{dtdp})]_n$ (CEBLUR01), containing μ-**dtdp** ligands of opposite chirality.

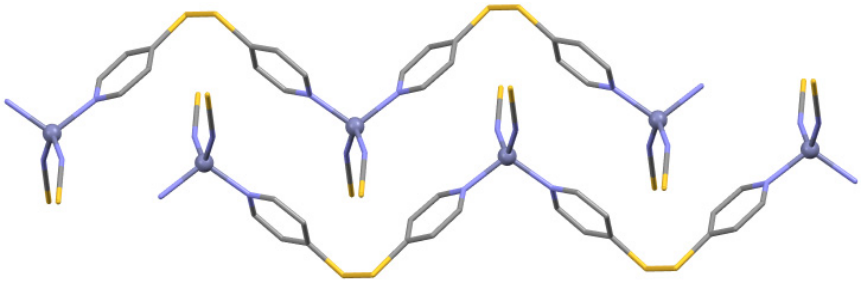

3.4. Zigzag and Helical Chains

Table 4 lists coordination polymers with zigzag and helical chain structure derived from **dtdp**. Since the border between these two basic structural motifs can become rather blurred, the related structures are discussed in one section. [*trans*-Mn(hfacac)$_2$(μ-**dtdp**)] (XEYTIE), the first example of a genuine zigzag chain structure containing **dtdp**, was reported by Horikoshi *et al.* in 2001 [50]. In XEYTIE, *trans*-configured Mn(hfacac)$_2$ units are joined by **dtdp** ligands of opposite chirality in an alternating fashion (Figure 15a). At around the same time, a structure comprising genuine helical chains with the composition [Cu(hfacac)$_2$(μ-**dtdp**)]$_n$ (XEYTEA) was reported [45,50]. The helical chains in XEYTEA consist of *cis*-configured Cu(hfacac)$_2$ units joined by **dtdp** linkages of the same chirality (Figure 15b). The helices so formed propagate by 2_1 screw symmetry in the crystal and exhibit a handedness opposite to the chirality of the *cis*-Cu(hfacac)$_2$ and **dtdp** building blocks. XEYTIE and XEYTEA were obtained under similar conditions, that is, from a mixture of **dtdp** and the M(hfacac)$_2$·2H$_2$O (M = Cu, Mn) precursor in methanol. The helical supramolecular isomer of XEYTIE, [*cis*-Mn(hfacac)$_2$(μ-**dtdp**)]$_n$ (XEYTIE01), which is isotructural with XEYTEA (M = Cu), crystallised from a solution of [Mn(hfacac)$_2$(H$_2$O)] and **dtdp** in a mixture of tetrachloromethane and dietheylether. Owing to the lability towards ligand substitution, M(hfacac)$_2$ precursors with 3d metal ions can undergo *cis*-*trans* isomerisation during the crystallisation. Reaction of Cu(hfacac)$_2$·2H$_2$O and **dtdp**, however, led to the helical chain structure, regardless of the solvent system studied [86]. XEYTIE and XEYTIE01 represent a remarkable example of supramolecular isomerism induced by the solvent system, all the more notable because solvent guest molecules were not encountered in the final outcome of crystallisation. As reported in Section 3.1, M_2L_2 macrocycles were obtained from [Co(hfacac)$_2$(H$_2$O)$_2$] and [Ni(hfacac)$_2$(H$_2$O)] and **dtdp**, independent of the solvent system used.

Table 4. Selected structural parameters for zigzag and helical chains.

Compound	C–S–S–C torsion angle (°)	M···M separation (Å)	Reference	CSD Refcode
[*trans*-Mn(hfacac)$_2$(μ-dtdp)]$_n$ [a]	90.9	11.79	[50]	XEYTIE
[*cis*-Mn(hfacac)$_2$(μ-dtdp)]$_n$ [a]	90.1	11.47	[48]	XEYTIE01
[Cu(hfacac)$_2$(μ-dtdp)]$_n$ [a]	91.9	11.26	[45,50]	XEYTEA
[Ni(C$_8$H$_{10}$O$_2$PS$_2$)$_2$(μ-dtdp)]$_n$ [b]	71.4	9.73	[87]	NIPVUE
[Cu(CH$_3$COO)$_2$(μ-dtdp)·6H$_2$O]$_n$	not available		[86]	PAWCAS
[Zn(C$_6$H$_{14}$O$_2$PS$_2$)$_2$(μ-dtdp)]$_n$ [c]	90.2	11.04	[88]	VEDDAK
[{Ag(μ-dtdp)}NO$_3$·0.5CH$_3$CN]$_n$	83.2	10.15	[89]	EDOHEK
[{Ag(μ-dtdp)}C$_7$H$_7$SO$_3$]$_n$ [d]	96.2	10.44	[89]	EDOHAG

[a] hfacac$^-$ = 1,1,1,5,5,5-hexafluoroacetylacetonate; [b] C$_8$H$_{10}$O$_2$PS$_2^-$ = *O*-methyl(4-methoxyphenyl)-phosphonodithionate; [c] C$_6$H$_{14}$O$_2$PS$_2^-$ = *O*,*O*′-diisopropyldithiophosphate; [d] C$_7$H$_7$SO$_3^-$ = 4-toluenesulfonate.

The coordination polymer strands in [Ni(C$_8$H$_{10}$O$_2$PS$_2$)$_2$(μ-**dtdp**)]$_n$ (NIPVUE) (C$_8$H$_{10}$O$_2$PS$_2$ = *O*-methyl(4-methoxyphenyl)phosphonodithioate) [87] can be regarded as an intermediate between zigzag and helical chain (Figure 16). Each single strand in the centrosymmetric crystal structure is composed of **dtdp** ligands of the same chirality and *trans*-configured Ni(C$_8$H$_{10}$O$_2$PS$_2$)$_2$ units as linear connectors. The chains thus formed extend by 2_1 screw symmetry in the crystal. The C–S–S–C torsion

angle deviates remarkably from the ideal 90°, indicating that there is some strain in the structure. In contrast to XEYTEA and XEYTIE01, the helicity of the strands in NIPVUE exhibits the same handedness as the **dtdp** ligands they are built from.

Figure 15. (**a**) Achiral zigzag chain structure in [*trans*-Mn(hfacac)$_2$(μ-**dtdp**)] (XEYTIE); (**b**) Helical chain structure in [Cu(hfacac)$_2$(μ-**dtdp**)]$_n$ (XEYTEA), showing the *P* form of **dtdp** and the Δ configuration of the *cis*-Cu(hfacac)$_2$ units. The helix so formed is, however, left-handed.

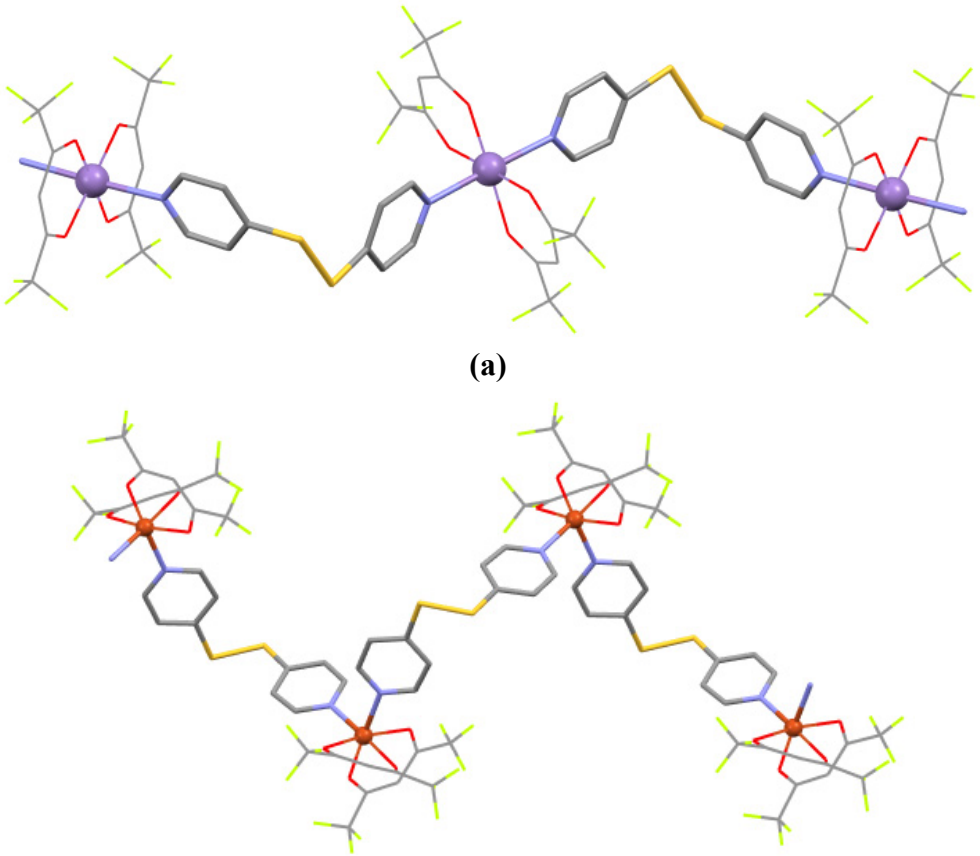

(a)

(b)

Figure 16. Coordination polymer strand in [Ni($C_8H_{10}O_2PS_2$)$_2$(μ-**dtdp**)]$_n$ (NIPVUE), showing the *P* form of **dtdp**.

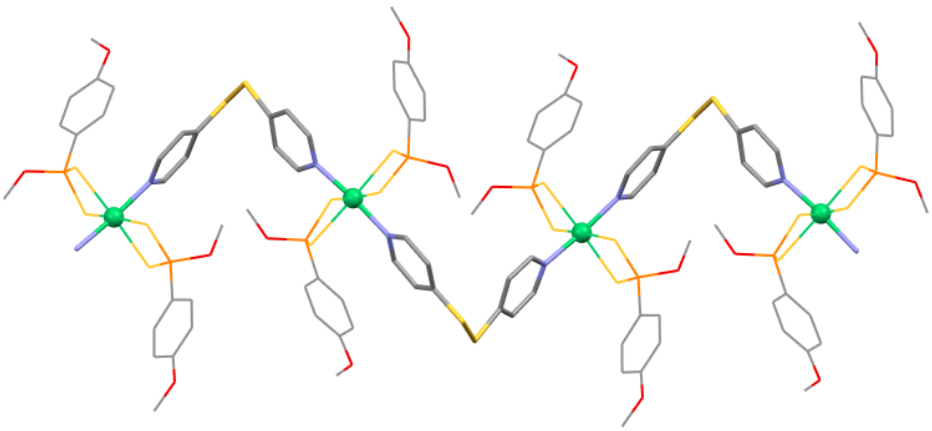

$[Cu(CH_3COO)_2(\mu\text{-}\mathbf{dtdp})\cdot 6H_2O]_n$ (PAWCAS) represents a zigzag chain similar to XEYTIE, where **dtdp** ligands of opposite handedness are connected by *trans*-$Cu(CH_3COO)_2$ units, serving as linear connectors. The structure has been described by Horiksohi and Mikuryia, but three-dimensional coordinates of the crystal structure have not been published [86]. As reported in Section 3.3, an analogous Zn(II) coordination polymer (FAYQUS) exhibits the arched chain structure, in which the Zn(II) ions are in a tetrahedral coordination environment with monodentate-bound acetato ancillary ligands. Coordination polymers of **dtdp** with multinuclear nodes derived from copper(II) acetate are described in Section 3.6.

$[Zn(C_6H_{14}O_2PS_2)_2(\mu\text{-}\mathbf{dtdp})]_n$ (VEDDAK) ($C_6H_{14}O_2PS_2^-$ = isopropyldithiophosphonate) can be seen as a distorted version of a zigzag chain (Figure 17) [88]. The chains in VEDDAK are composed of **dtdp** building blocks of opposite chirality in an alternating fashion joined by tetrahedrally coordinated Zn(II) ions with two monodentate bound isopropyldithiophosphonato ancillary ligands. As described in Section 3.3, an arched chain (BILFAE) is formed from **dtdp** and the heavier group homologue Cd(II) with the same co-ligands but there acting as bidentate chelate ligands.

Figure 17. Distorted zigzag chain in $[Zn(C_6H_{14}O_2S_2)_2(\mu\text{-}\mathbf{dtdp})]_n$ (VEDDAK), showing an $M–L_P–M–L_M–M–L_P–M–L_M–M$ sequence.

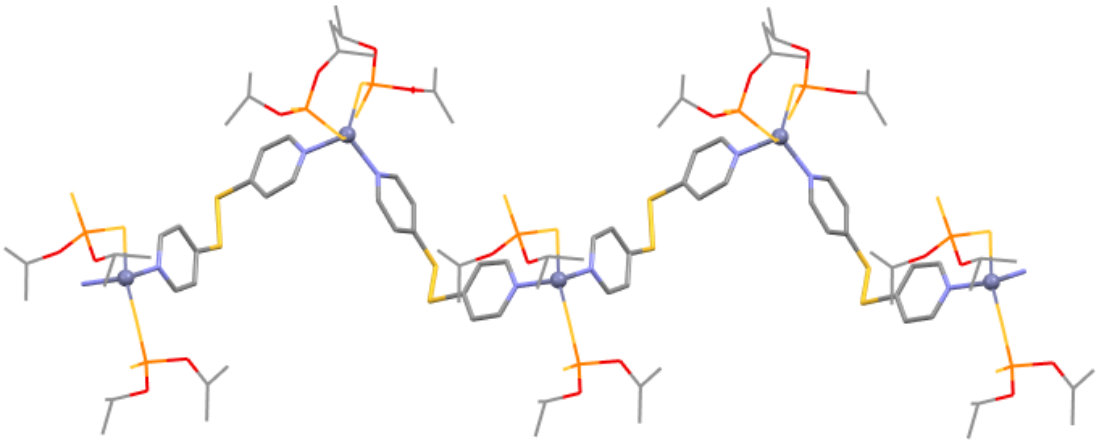

In 2002, Horikoshi *et al.* described the preparation and structural characterisation of a series of coordination polymers from **dtdp** and silver(I) salts [89]. An intermediate zigzag/helical chain was obtained from $AgNO_3$ and a zigzag chain structure with Ag–Ag cross-links was isolated in the presence of 4-toluenesulfonate counter-ions, whereas silver(I) hexafluorophosphate and perchlorate afforded two-dimensional coordination networks with (4,4) net topology (see Section 3.5). In $[\{Ag(\mu\text{-}\mathbf{dtdp})\}NO_3\cdot 0.5CH_3CN]_n$ (EDOHEK), Ag(I) ions adopt a characteristic two-coordination, connecting two **dtdp** building blocks in an almost linear fashion (Figure 18a). All **dtdp** ligands in a single strand are of the same chirality. In the crystal, the chains thus formed extend by 2_1 screw symmetry. Similar to NIPVUE, the coordination polymer strands in EDOHEK are best described as intermediate between zigzag and helical chains. Likewise, the helicity of the entire strands is the same as that of the **dtdp** building blocks. The strands of the same handedness are tightly packed to form layers. Layers of opposite handedness stack in an alternating fashion, with nitrate ions linking the coordination polymer at Ag(I) (Figure 18b). Acetonitrile guest molecules fill the voids. In $[\{Ag(\mu\text{-}\mathbf{dtdp})\}C_7H_7SO_3]_n$ (EDOHAG), alternating **dtdp** building blocks of opposite chirality are connected by Ag(I) ions in a

nearly linear fashion to form zigzag chains, which are cross-linked by *inter*chain Ag–Ag bonds (Ag–Ag distance: 3.05 Å). The Ag(I) ions adopt a T-shaped coordination geometry (Figure 18c). EDOHAG thus in fact represents a two-dimensional coordination network. In the crystal, the sheets so formed stack with layers of 4-toluenesulfonate in between.

Figure 18. (**a**) Compact arrangement of two adjacent strands in $[\{Ag(\mu\text{-}\mathbf{dtdp})\}NO_3 \cdot 0.5CH_3CN]_n$ (EDOHEK), showing the *P* form **dtdp**; (**b**) Opposite-handed strands of EDOHEK linked by nitrate ions at Ag(I); (**c**) Adjacent zigzag chains in $[\{Ag(\mu\text{-}\mathbf{dtdp})\}C_7H_7SO_3]_n$ (EDOHAG) with Ag–Ag (d^{10}–d^{10}) cross-links, showing $M–L_P–M–L_M–M–L_P–M$ sequences in the chains.

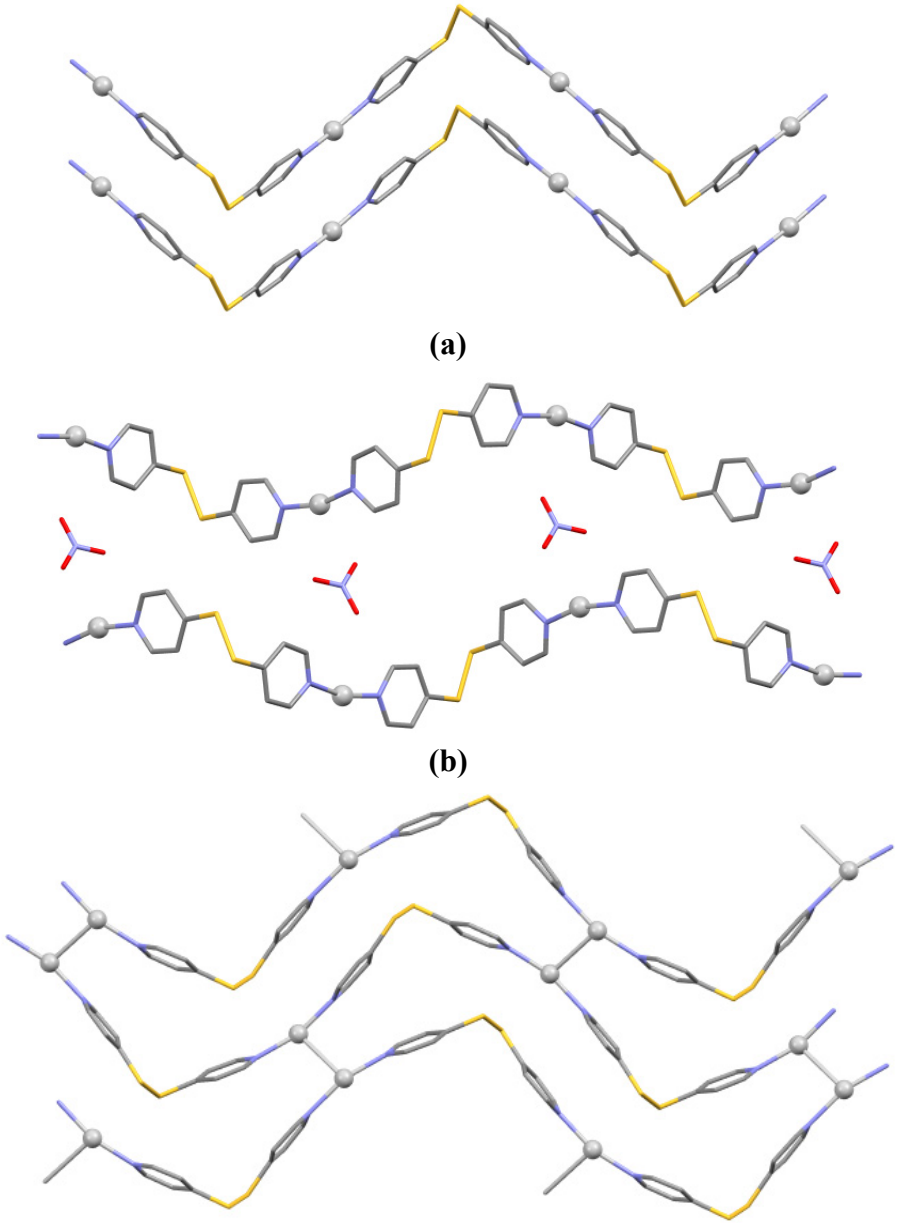

(a)

(b)

(c)

3.5. Coordination Networks with (4,4) Net Topology

As mentioned in the previous section, Horikoshi *et al.* obtained two-dimensional coordination networks with (4,4) net topology from **dtdp** and silver(I) hexafluorophosphate and perchlorate, whereas the nitrate and 4-methanetoluenesulfonate afforded respectively an intermediate zigzag/helical chain structure and a zigzag chain structure with Ag–Ag cross-links. In $[\{Ag(\mu\text{-}\mathbf{dtdp})_2\}PF_6]_n$ (EDOGOT) and $[\{Ag(\mu\text{-}\mathbf{dtdp})_2\}ClO_4]_n$ (EDOGUZ) the Ag(I) ions adopt a tetrahedral coordination geometry with four pyridyl groups of **dtdp** serving as four-connecting nodes to form distorted (4,4) net structures. The cationic coordination networks in EDOGOT and EDOGUZ are isostructural; Figure 19 depicts the representative structure of the former. Crystallographic twofold rotation axes run through the Ag(I) ions, and the asymmetric unit contains one **dtdp** ligand. The shortest circuit back to a starting Ag(I) four-connecting node contains four symmetry-related **dtdp** ligands of the same chirality. Alternate layers contain **dtdp** ligands of opposite handedness. The C–S–S–C torsion angles are ±91.4° in EDOGOT and ±90.3° in EDOGUZ. The corresponding Ag···Ag non-bonding distances are 11.35 Å in EDOGOT and 11.14 Å in EDOGUZ. The increased C–S–S–C torsion angle and Ag···Ag distance in EDOGOT as compared to EDOGUZ can be attributed to the presence of the bulkier hexafluorophospate counter-ions in the voids of EDOGOT.

Figure 19. Coordination network with (4,4) net topology in $[\{Ag(\mu\text{-}\mathbf{dtdp})_2\}PF_6]_n$ (EDOGOT).

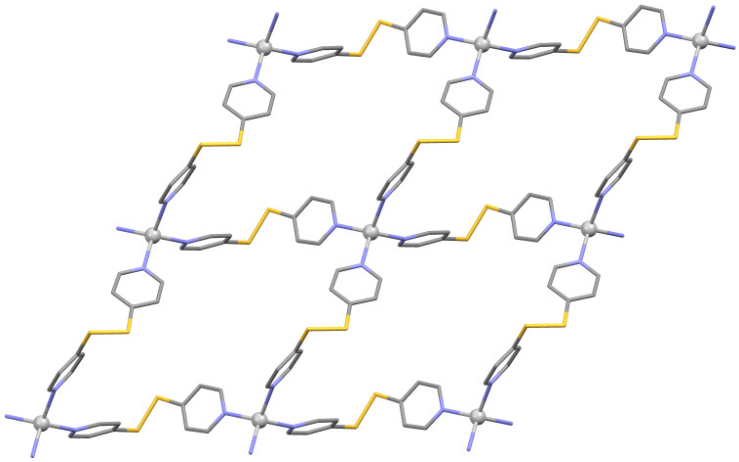

Layering a solution of cadmium(II) chloride in a methanol/water mixture onto a solution of **dtdp** in acetonitrile yielded colourless crystals of $[CdCl_2(\mu\text{-}\mathbf{dtdp})_2]_n$ (EMADAX) [61]. The structure of EMADAX is a distorted (4,4) net comprising *trans*-octahedral $CdCl_2$ four-connecting nodes and **dtdp** linkages (Figure 20). The Cd(II) ions reside on crystallographic centres of symmetry, and the structure contains one crystallographically unique **dtdp** ligand (C–S–S–C torsion angle: 95.0°). The sequence of conformations of the four symmetry-related **dtdp** ligands forming the shortest route to complete a circuit back to a starting *trans*-$CdCl_2$ node is *MMPP*. The Cd···Cd separation in a sheet is 12.27 Å. Since the four equatorial pyridyl groups of the **dtdp** ligands are bound to Cd(II) are approximately orthogonal to one another (N–Cd–N: 83.8° and 95.2°), the (4,4) net layers in EMADAX are not as corrugated as in EDOGOT and EDOGUZ, where the Ag(I) ions are tetrahedrally coordinated. It is worth noting that in all three cases the metal atoms in a net layer are coplanar.

Figure 20. Coordination network with (4,4) net topology in $[CdCl_2(\mu\text{-}\mathbf{dtdp})_2]_n$ (EMADAX).

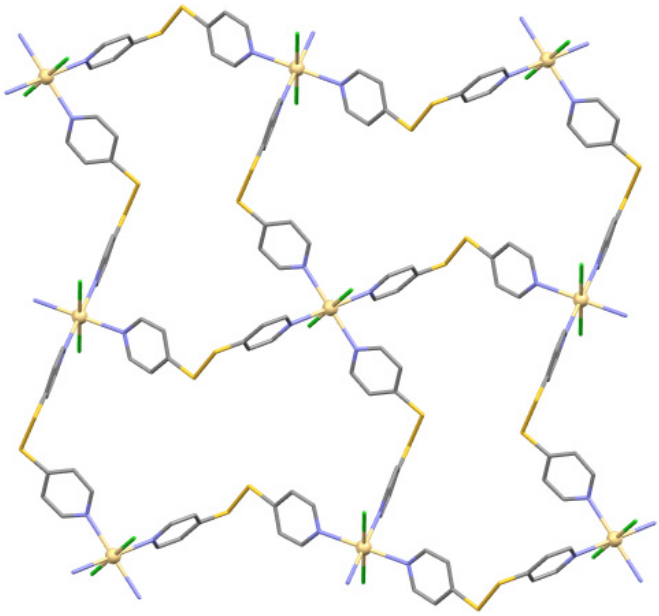

3.6. Coordination Polymers Based on Metal Carboxylate Clusters

This section describes coordination polymers containing the **dtdp** ligand and metal carboxylate clusters as nodes. Table 5 lists relevant structures, roughly sorted by complexity and increasing atomic number of the metal ions involved. $[Co_3(\mu_3\text{-}OH)(tbip)_2(Htbip)(\mu\text{-}C_{10}H_8N_2S)(\mu\text{-}\mathbf{dtdp})_{0.5}]_n$ (GUXPIZ, $tbip^{2-}$ = 5-*tert*-butylisophthalate, $C_{10}H_8N_2S$ = 4,4′-dipyridylsulfide) was obtained by the reaction of $Co(CH_3COO)_2{\cdot}4H_2O$ with H_2tbip in a methanol/acetonitrile mixture [90]. The 4,4′-dipyridylsulfide bridging ligand encountered in the structure results from partial *in situ* S–S and C–S cleavage and rearrangement reactions of **dtdp**. GUXPIZ represents a three-dimensional coordination network. Figure 21 depicts a characteristic unit of the structure. The nodes are formed by trinuclear μ_3-hydroxido-bridged Co(II) clusters. Four bidentate μ-carboxylate groups, a monodentate-bound carboxylate group, a monodenate-bound neutral carboxyl group as well as three pyridyl groups are attached to the cluster. The crystal structure of GUXPIZ is chiral with orthorhombic $P2_12_12$ space group symmetry. It has not been reported whether the bulk sample was enantiopure or whether the compound crystallised as a conglomerate, although this is more likely in the absence of an external source of chirality. As shown in Figure 21, two nodes are triply joined by two $Htbip^-$ ligands and a **dtdp** ligand exhibiting the right-handed *P* conformation. The C–S–S–C torsion angle of **dtdp** is remarkably small (Table 5), which can be attributed to the fact that the M···M distance is dictated by the $Htbip^-$ ligands. A crystallographic twofold rotation axis parallel to the [001] direction runs through the centre of the disulfide moiety. In this direction, the trinuclear Co(II) nodes are doubly bridged by an *in situ* formed 4,4′-dipyridylsulfide and a $tbip^{2-}$ ligand. Another $tbip^{2-}$ ligand links a node to an ajdacent node in the [100] direction. Thus, each trinuclear Co(II) cluster can be viewed as a five-connecting node. The overall topolgy of the resulting three-dimensional coordination network has been described as a boron nitride (**bnn**) type [91]. Magnetic susceptibility measurements revealed ferromagnetic coupling within the trinuclear Co(II) nodes.

Table 5. Selected structural parameters for coordination polymers based on metal carboxylate clusters.

Compound	C–S–S–C torsion angle (°)	M···M separation (Å) [a]	Reference	CSD Refcode
$[Co_3(\mu_3\text{-OH})(tbip)_2(Htbip)(\mu\text{-}C_{10}H_8N_2S)(\mu\text{-dtdp})_{0.5}]_n$ [b]	72.5	7.94	[90]	GUXPIZ
$[Cu_2(CH_3COO)_4(\mu\text{-dtdp})]_n$ [c]	89.6	11.39	[92]	LIGPOH
$[Cu_2(C_6H_5COO)_4(\mu\text{-dtdp})]_n$ [d]	86.5	10.62	[86]	PAWBOF
$[Cu_2(C_5H_{11}COO)_4(\mu\text{-dtdp})]_n$ [e]	90.6, −91.8	11.34, 11.42	[86]	PAWBUL
$[Cu_4(CH_3COO)_6(\mu_3\text{-OH})_2(\mu\text{-dtdp})_2]_n$	81.3, 83.2	9.79, 9.90	[86]	PAWBIZ
$[Cu_4(HCOO)_6(\mu_3\text{-OH})_2(\mu\text{-dtdp})_2\cdot CH_2Cl_2]_n$	75.3	9.40	[64]	VUKFUD
$[\{Cu_2(\mu\text{-}C_2O_4)(H_2O)_4(\mu\text{-dtdp})_2\}(ClO_4)_2]_n$	79.5	9.94	[93]	RIRSOB
$[Cu(malate)(\mu\text{-dtdp})\cdot 6H_2O]_n$	90.3	10.68	[94]	MEFMEQ
$[Zn_7(CH_3COO)_{10}(\mu_4\text{-O})_2(\mu\text{-dtdp})]_n$	85.5	10.43	[95]	VAKZIR

[a] Refers to the M···M separation through the **dtdp** ligand; [b] $tbip^{2-}$ = 5-*tert*-butylisophthalate, $C_{10}H_8N_2S$ = 4,4′-dipyridylsulfide; [c] The crystal structure contains solvent accessible voids (see text); [d] $C_6H_5COO^-$ = benzoate; [e] $C_5H_{11}COO^-$ = hexanoate.

Figure 21. Section of the crystal structure of $[Co_3(\mu_3\text{-OH})(tbip)(Htbip)(\mu\text{-}C_{10}H_8N_2S)(\mu\textbf{-dtdp})_{0.5}]_n$ (GUXPIZ), viewed approximately along the [100] direction. A crystallographic twofold rotation axis parallel to [001] bisects the **dtdp** moiety.

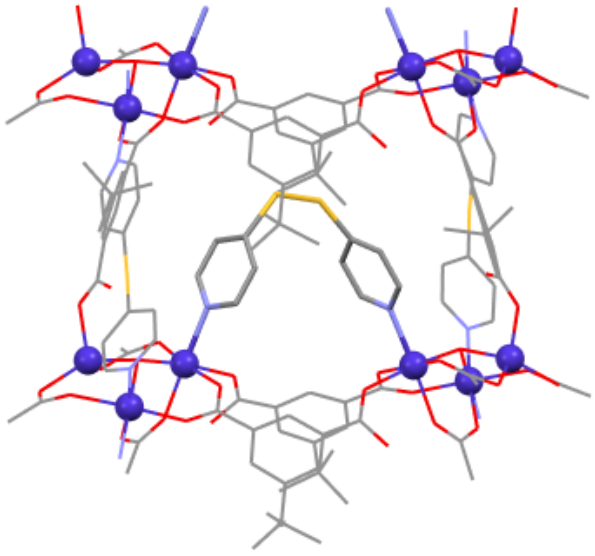

Three one-dimensional coordination polymers based on **dtdp** and the well-known metal carboxylate paddle-wheel synthon [96] have been reported. $[Cu_2(CH_3COO)_4(\mu\textbf{-dtdp})]_n$ (LIGPOH) was obtained from $Cu(CH_3COO)_2\cdot H_2O$ and **dtdp** in methanol [92]. The structure features zigzag chains assembled from dinuclear copper(II) actetate paddle-wheel units as linear connectors joined by **dtdp** ligands in the *P* and *M* conformation in an alternating fashion (Figure 22). The one-dimensional coordination polymer strands are thus topologically similar to the zigzag chain with mononuclear, linear *trans*-$Mn(hfacac)_2$ nodes (XEYTIE), described in Section 3.4. The crystal structure of LIGPOH exhibits orthorhombic symmetry (space group *Pccn*). The paddle-wheel unit contains a crystallographic centre of symmetry and the **dtdp** ligand a twofold rotation axis passing through the centre of the

disulfide moiety. In the crystal, adjacent zigzag chains that are crossed extend in the [110] and [1$\bar{1}$0] directions, thereby generating open channels parallel to the [001] direction. It should be mentioned that the crystal structure of LIGPOH reported by Delgado *et al.*, contains solvent accessible voids of *ca.* 166 Å^3 per unit cell volume. The reported description of LIGPOH as a solvent-free crystal structure is therefore questionable. $[Cu_2(C_6H_5COO)_4(\mu\text{-}\mathbf{dtdp})]_n$ (PAWBOF) and $[Cu_2(C_5H_{11}COO)_4(\mu\text{-}\mathbf{dtdp})]_n$ (PAWBUL) exhibit a similar zigzag chain structure as LIGPOH, but the paddle-wheel units are formed from copper(II) benzoate in PAWBOF and hexanoate in PAWBUL [86]. The paddle-wheel unit in PAWBOF is located on a crystallographic inversion centre similar to LIGPOH. The asymmetric unit of PAWBUL contains two repeat units in one zigzag chain. PAWBUL thus can be regarded as a $Z' = 2$ crystal structure [76,77]. The packing of the zigzag chains in PAWBOF and PAWBUL is different from LIGPOH. In PAWBOF and PAWBUL the zigzag chains run parallel in the [$\bar{1}$11] and [101] direction of the triclinic and monoclinic unit cells, respectively. Temperature-dependent measurements of the magnetic susceptibility of LIGPOH and PAWBOF revealed strong antiferromagnetic coupling, as expected for dinuclear copper(II) carboxylate units.

Figure 22. Achiral zigzag chain structure in $[Cu_2(CH_3COO)_4(\mu\text{-}\mathbf{dtdp})]_n$ (LIGPOH).

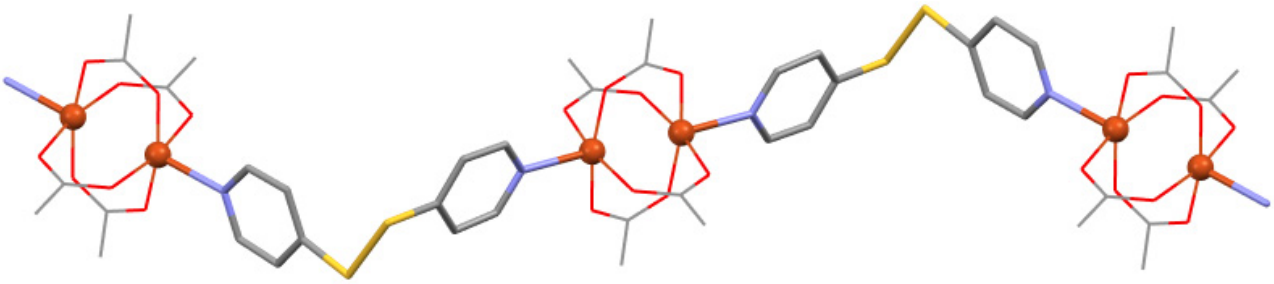

$[Cu_4(CH_3COO)_6(\mu_3\text{-}OH)_2(\mu\text{-}\mathbf{dtdp})_2]_n$ (PAWBIZ) and $[Cu_4(HCOO)_6(\mu_3\text{-}OH)_2(\mu\text{-}\mathbf{dtdp})_2]_n$ (VUKFUD) represent two ribbon structures based on similar tetranuclear μ_3-hydroxido-bridged copper(II) carboxylate nodes (Figure 23). Crystals of PAWBIZ were obtained by recrystallisation of an initial pale-green precipitate resulting from the reaction of **dtdp** and $Cu(CH_3COO)_2{\cdot}H_2O$ in methanol [86]. It is interesting to note that recrystallisation of the raw product or crystals of PAWBIZ from water gave blue crystals of PAWCAS, which exhibts an achiral zigzag chain structure with mononuclear copper(II) actetate nodes (see Section 3.4). VUKFUD resulted from mixing a solution of $Cu(HCOO)_2{\cdot}H_2O$ in methanol with a solution of **dtdp** in dichloromethane [64]. The constitution of the tetranuclear basic copper(II) carboxylate clusters is essentially similar in PAWBIZ and VUKFUD. The inner core consists of a central Cu_2O_2 ring and two lateral Cu(II) ions, each bonded to oxygen, so that two μ_3-hydroxido ions link the two inner and two lateral Cu(II) ions. In addition, the cluster contains four μ-briding bidentate and two monodentate carboxylate groups bound to the lateral Cu(II) ions. In VUKFUD, the tetranuclear clusters contain a crystallographic centre of symmetry. In both PAWBIZ and VUKFUD, the tetranuclear clusters are linked by two **dtdp** ligands into one-dimensional coordination polymer strands, which resemble the repeated rhomboid structure, described in Section 3.2. In PAWBIZ, the macrocyclic units built from two nodes and two **dtdp** ligands each contain only one conformational enantiomer of the ligand, but *P* and *M* forms generate the macrocyclic units in an alternating fashion (Figure 23a). In VUKFUD, the macrocyclic units are built from **dtdp** ligands of

opposite chirality and exhibt crystallographic inversion symmetry (Figure 23b). It is worth noting that the chains in PAWBIZ are more ruffled than those in VUKFUD, as revealed by Figure 23.

Figure 23. Repeated rhomboid related coordination polymer strands based on tetranuclear basic copper(II) carboxylate nodes in (**a**) $[Cu_4(CH_3COO)_6(\mu_3\text{-}OH)_2(\mu\text{-}\mathbf{dtdp})_2]_n$ (PAWBIZ) and (**b**) $[Cu_4(HCOO)_6(\mu_3\text{-}OH)_2(\mu\text{-}\mathbf{dtdp})_2]_n$ (VUKFUD).

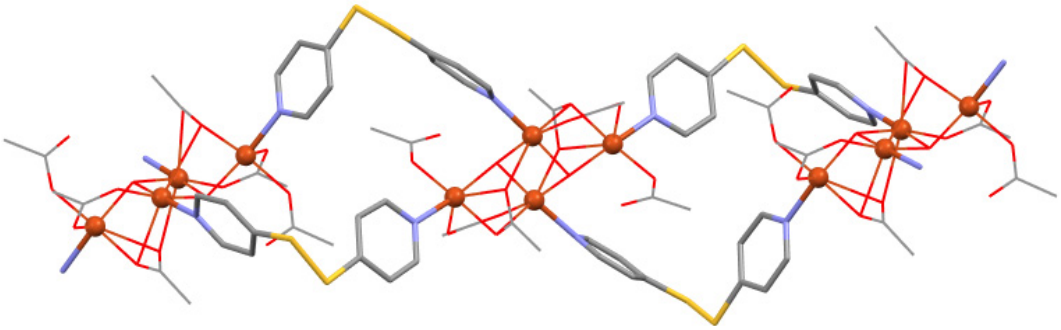

(a)

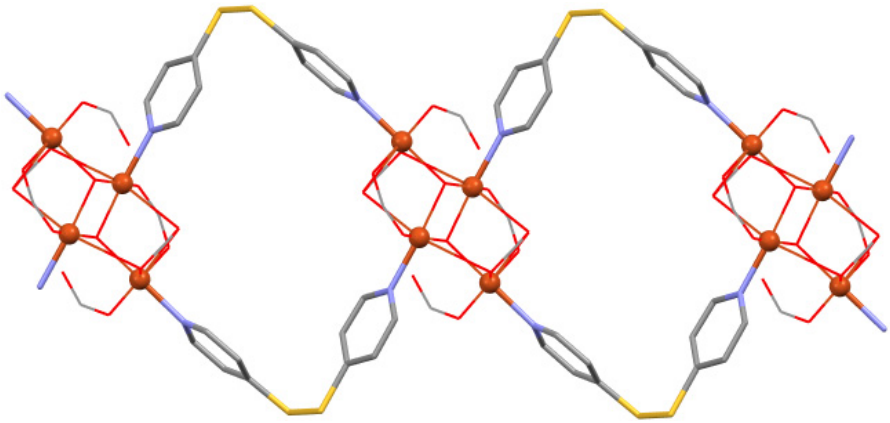

(b)

$[\{Cu_2(\mu\text{-}C_2O_4)(H_2O)_4(\mu\text{-}\mathbf{dtdp})_2\}(ClO_4)_2]_n$ (RIRSOB) [93] and $[Cu(malate)(\mu\text{-}\mathbf{dtdp})\cdot 6H_2O]_n$ (MEFMEQ) [94] contain multinuclear nodes composed of Cu(II) and dicarboxylic acid dianions, namely oxalate and malate, respectively. Figure 24 shows the ribbon structure of a coordination polymer strand in RIRSOB. The structure is closely related to the chiral repeated rhomboids, described in Section 3.2. The μ-oxalato ligands bridge two Cu(II) ions each in a bidentate chelate coordination mode, thereby occupying two *cis* coordination sites in the equatorial planes of the two Cu(II) centres. The dinuclear nodes so formed are linked by two **dtdp** ligands of the same chirality to form repeated-rhomboid-like chains. Aqua ligands in apical positions complete the octahedral coordination sphere of the Cu(II) ions. At both the centre of the oxalate C–C bond and the centre of the chiral macrocyclic unit, the site symmetry in the crystal structure is 222 (orthorhombic *Fddd* space group symmetry).

MEFMEQ was prepared from copper(II) malate and **dtdp**, using a water/ethanol solvent system. The structure is illustrated in Figure 25. The dianion of malic acid acts as a chelate ligand, coordinating to three facial coordination sites of Cu(II). The 2-hydroxy group and the monodentate-bound 1-carboxylate group form a five-membered chelate ring in the equatorial plane of the Cu(II) coordination sphere. The 4-carboxylate group is monodentate-bound to an axial coordination site. The Cu(malate) units are joined by **dtdp** via the remaining two equatorial *cis* sites to form an

arched chain, extending in the [100] direction of the monoclinic structure (space group $P2_1/n$). In the [010] direction, chains that are symmetry-related by a 2_1 screw operation are connected through the second oxygen atom of the 4-carboxylate group, which coordinates to the remaining axial coordination site of Cu(II) in the adjacent chain. Thus, the structure does not in fact contain isolated metal carboxylate clusters but polymeric chains of μ-carboxylato-linked Cu(II) ions. The overall topology of the resulting two-dimensional coordination network can be regarded as a (4,4) net. The conformation of **dtdp** and the configuration of the malato ligand exhibit opposite chirality in adjacent (4,4) net layers. The crystal structure contains large circular holes, each containing 18 molecules of water.

Figure 24. Coordination polymer strand in $[\{Cu_2(\mu\text{-}C_2O_4)(H_2O)_4(\mu\text{-}\mathbf{dtdp})_2\}(ClO_4)_2]_n$ (RIRSOB), resembling a chiral repeated rhomboid structure.

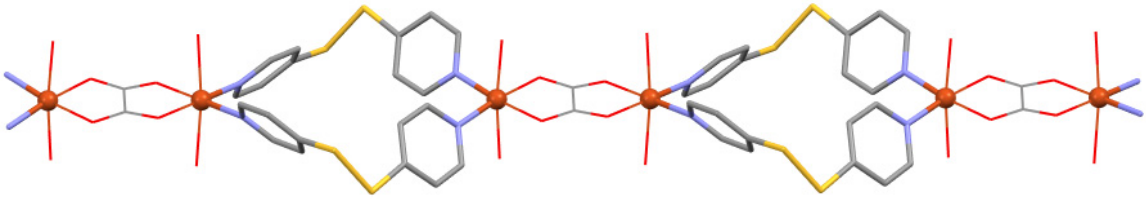

Figure 25. Coordination network in $[Cu(malate)(\mu\text{-}\mathbf{dtdp})\cdot 6H_2O]_n$ (MEFMEQ), showing the right-handed *P* form of **dtdp** and the left-handed Cu(*S*-malate) units.

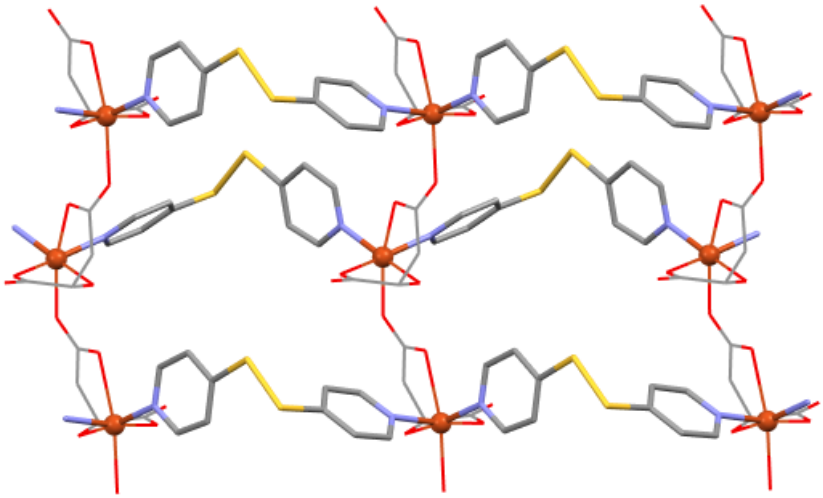

Reaction of **dtdp** and zinc(II) actetate in an acetonitrile/methanol solvent system resulted in $[Zn_7(CH_3COO)_{10}(\mu_4\text{-}O)_2(\mu\text{-}\mathbf{dtdp})]_n$ (VAKZIR) [95]. The structure features heptanuclear Zn(II) clusters joined alternately by **dtdp** ligands of opposite handedness to form an achiral zigzag chain structure (Figure 26). The heptanuclear Zn(II) clusters each contain ten μ-acetato and two μ_4-oxido ligands. The inner Zn_3–O–Zn–O–Zn_3 core adopts a D_{3d}-symmetric local structure and the Zn(II) ions are further connected by the μ-acetato ligands. The central Zn(II) ion resides on a centre of symmetry in the crystal structure and exhibits an octahedral coordination sphere. The coordination environment of the two Zn(II) ions bearing the pyridyl groups of **dtdp** is also octahedral, whereas that of the remaining four Zn(II) ions is tetrahedral.

Figure 26. Achiral zigzag chain structure in $[Zn_7(CH_3COO)_{10}(\mu_4\text{-}O)_2(\mu\text{-}\mathbf{dtdp})]_n$ (VAKZIR), featuring heptanuclear basic Zn(II) acetate clusters as nodes.

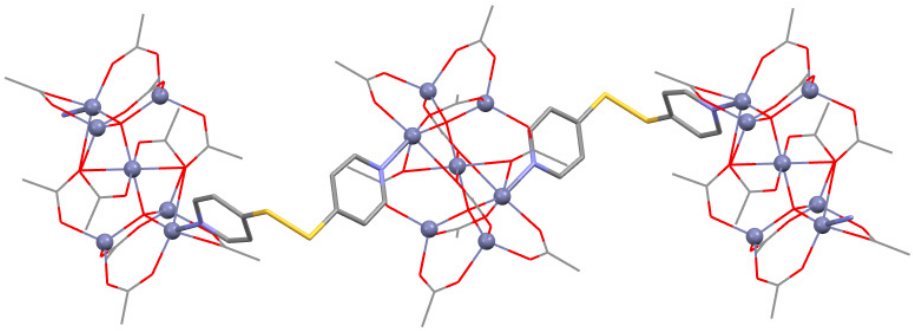

3.7. Coordination Polymers Based on Metal Sulfide or Metal Iodide Clusters

This section deals with **dtdp**-based coordination polymers that contain metal sulfide or metal iodide clusters as nodes; Table 6 summarises relevant structures. Lang *et al.* have described the preparation and structural characterisation of two Mo/Cu/S or W/Cu/S cluster-based coordination polymers with **dtdp** bridges [97]. Reaction of the cluster precursor $(n\text{-}But_4N)_2[MoOS_3Cu_3I_3]$ (But = butyl) with **dtdp** in a mixture of *N*,*N*-dimethylformamide (DMF) and acetonitrile afforded $[MoOS_3Cu_3I(\mu\text{-}\mathbf{dtdp})_2\cdot 0.5DMF\cdot CH_3CN]_n$ (KEXDOH), and treatment of a solution of $(n\text{-}But_4N)_2[WS_4Cu_4I_6]$ in acetonitrile with a solution of **dtdp** and sodium dicyanamide (dca) in methanol yielded $[WS_4Cu_4(\mu\text{-dca})_2(\mu\text{-}\mathbf{dtdp})_2\cdot Et_2O\cdot 2CH_3CN]_n$ (KEXDIB) upon slow diffusion of diethylether into the mixture. KEXDOH contains one-dimensional coordination polymer strands (Figure 27). The nodes are provided by *nido*-like $MoOS_3Cu_3$ clusters, in which the μ_3-sulfur atoms of the $[MoOS_3]^{2-}$ anion connect the three copper atoms. Each two **dtdp** ligands of opposite handedness link the $MoOS_3Cu_3$ clusters into a one-dimensional coordination polymer, extending by 2_1 screw symmetry in the *b* axis direction. As shown in Figure 27, the coordination polymer strands can be regarded as repeated rhomboids (see Section 3.2) arranged in a zigzag manner. The C–S–S–C torsion angles deviate markedly from the ideal 90° (see Table 6). The coordination sphere of the two Cu atoms within each cluster node that are bonded to two pyridyl groups of **dtdp** is tetrahedral. The remaining Cu atom bears a terminal iodido ligand and exhibits a trigonal-planar coordination environment.

Figure 27. Coordination polymer strand in $[MoOS_3Cu_3I(\mu\text{-}\mathbf{dtdp})_2\cdot 0.5DMF\cdot CH_3CN]_n$ (KEXDOH), formed from *nido*-like $MoOS_3Cu_3$ clusters each joined by two **dtdp** ligands of opposite chirality.

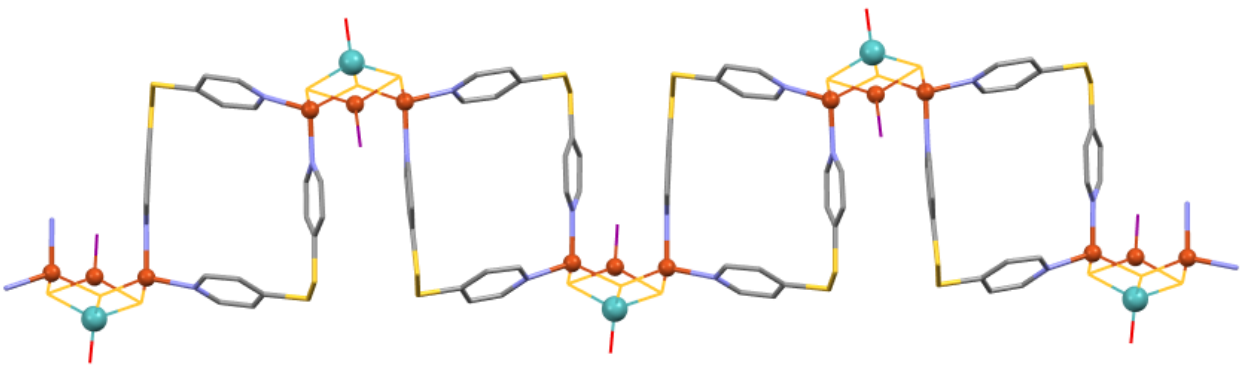

Table 6. Selected structural parameters for coordination polymers based on metal sulfide or metal iodide clusters.

Compound	C–S–S–C torsion angle (°)	M···M separation (Å) [a]	Reference	CSD Refcode
$[MoOS_3Cu_3I(\mu\text{-dtdp})_2\cdot 0.5DMF\cdot CH_3CN]_n$	80.4, −78.4	9.77	[97]	KEXDOH
$[WS_4Cu_4(\mu\text{-dca})_2(\mu\text{-dtdp})_2\cdot Et_2O\cdot 2CH_3CN]_n$ [b]	−84.4	10.52	[97]	KEXDIB
$[CuI(\mu\text{-dtdp})\cdot CH_3CN]_n$	83.6	10.64	[98]	ACAFIT
$[CuI(\mu\text{-dtdp})\cdot CH_2Cl_2]_n$	85.7	10.67	[98]	ACAFOZ
$[(CuI)_2(\mu\text{-dtdp})\cdot CH_3CN]_n$	88.5, −79.5	10.87, 9.86	[98]	ACAGAM
$[(CuI)_2(\mu\text{-dtdp})\cdot CH_3CH_2CN]_n$	77.4	9.29	[98]	ACAFUF

[a] Refers to the M···M separation through the **dtdp** ligand; [b] dca^- = dicyanamide.

KEXDIB represents a two-dimensional coordination network with a corrugated layer structure (Figure 28). Topologically, the structure can be described as a (4,4) net with $[WS_4Cu_4]^{2+}$ clusters serving as four-connecting nodes. Within the clusters, the central tungsten atom is tetrahedrally coordinated by four sulfur atoms, which act as μ_3-bridges to bind to the four lateral copper atoms. The tetrahedral coordination environment of the copper atoms is completed by a pyridyl group of **dtdp** and cyano group of the dicyanamido ligand. Each cluster node is doubly linked to four neighbouring nodes by a **dtdp** and a dicyanamido ligand. The layers so formed extend parallel to the *bc* plane of the orthorhombic unit cell. The compound was found to crystallise in the Sohncke space group $C222_1$ with a twofold rotation axis passing through the central tungsten atom of the cluster nodes parallel to the *a* axis direction. The Flack x parameter of 0.03(2) indicates that the crystal studied was enantiopure, containing the left-handed *M* form of **dtdp**, but no statement regarding the enantiopurity of the bulk sample was made.

Figure 28. Coordination network in $[WS_4Cu_4(\mu\text{-dca})_2(\mu\text{-}\mathbf{dtdp})_2\cdot Et_2O\cdot 2CH_3CN]_n$ (KEXDIB), viewed along the *a* axis direction.

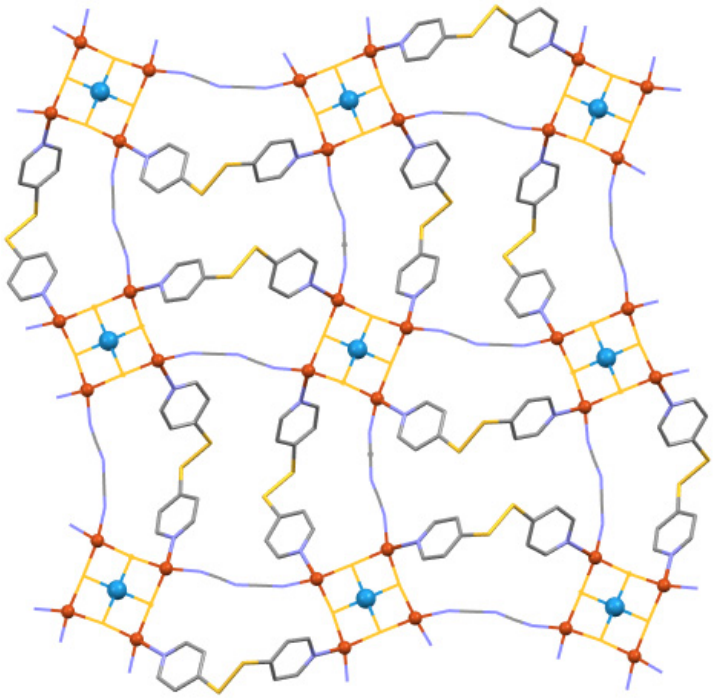

In 2001, Schröder and co-workers reported on neutral coordination networks formed from CuI clusters and **dtdp** [98]. Slow diffusion of a solution of CuI in acetonitrile or propionitrile into a solution of **dtdp** in dichloromethane gave yellow needles of $[CuI(\mu\text{-}\mathbf{dtdp})\cdot CH_3CN]_n$ (ACAFIT) or $[CuI(\mu\text{-}\mathbf{dtdp})\cdot CH_2Cl_2]_n$ (ACAFOZ) in the ligand-rich region and pale-yellow blocks of $[(CuI)_2(\mu\text{-}\mathbf{dtdp})\cdot CH_3CN]_n$ (ACAGAM) and $[(CuI)_2(\mu\text{-}\mathbf{dtdp})\cdot CH_3CH_2CN]_n$ (ACAFUF) in the metal-rich region. Both ACAFIT and ACAFOZ represent one-dimensional coordination polymers that have been labelled as planar ribbons and are topologically related to VUKFUD (Section 3.6). Figure 29 depicts the structure of a polymer chain in ACAFIT exemplary for both compounds. Cu_2I_2 four-membered rings serve as nodes and are joined by two **dtdp** ligands, which are related by crystallographic inversion symmetry. The structures thus resemble achiral repeated rhomboids (Section 3.2). The coordination sphere of the copper(I) ions is tetrahedral and comprises two μ-iodido ligands and two pyridyl groups of **dtdp**. ACAFUF and ACAGAM both contain cubane-like Cu_4I_4 clusters as nodes, which are linked by **dtdp** to form necklace chains in the first case and tubular chains in the latter (Figure 30). The coordination sphere of the copper(I) ions in the cluster nodes is tetrahedral in each case, formed by three iodido ligands and a pyridyl group of **dtdp**. In contrast to the planar ribbons in ACAFIT and ACAFOZ, the macrocyclic units in the necklace chains in ACAFUF are tilted to one another by *ca.* 88° (based on the two Cu and four N atoms in each macrcocycle). In the tubular chains in ACAGAM, Cu_4I_4 nodes are also linked by two **dtdp** ligands to form macrocyclic entities, but these are now interlinked by two further **dtdp** ligands. In both ACAFUF and ACAGAM, the polymer chains contain crystallographic centres of symmetry. It is worth pointing out that the ratio of Cu_4I_4 nodes and bridging ligands is the same in ACAFUF and ACAGAM. The two coordination polymers are thus supramolecular isomers, the actual structure of which depends on the solvent system used for crystallisation. In the crystals, solvent molecules are located in the cavities of the chains in both structures.

Figure 29. Coordination polymer strand in $[CuI(\mu\text{-}\mathbf{dtdp})\cdot CH_3CN]_n$ (ACAFIT), resembling an achiral repeated rhomboid structure.

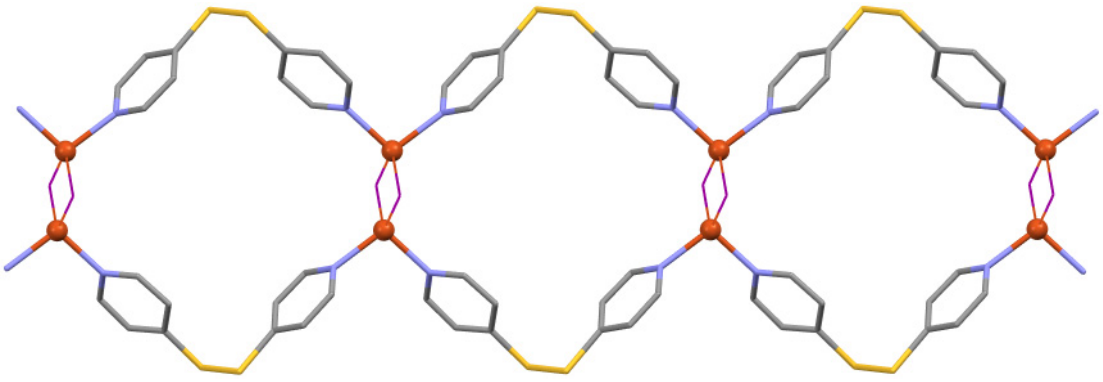

Figure 30. (**a**) Necklace chain in $[(CuI)_2(\mu\text{-}\mathbf{dtdp})\cdot CH_3CH_2CN]_n$ (ACAFUF); (**b**) Tubular chain in $[(CuI)_2(\mu\text{-}\mathbf{dtdp})\cdot CH_3CN]_n$ (ACAGAM).

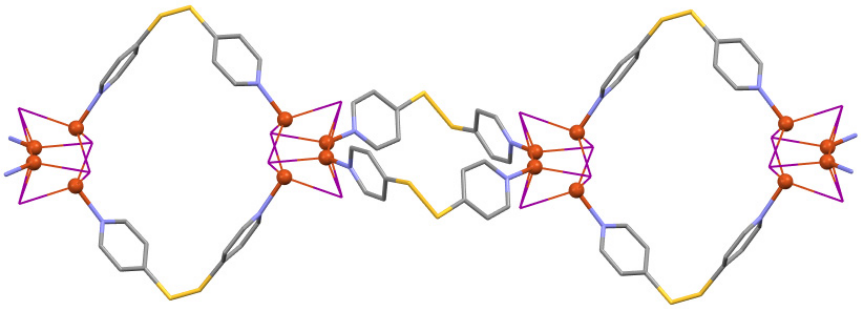

(a)

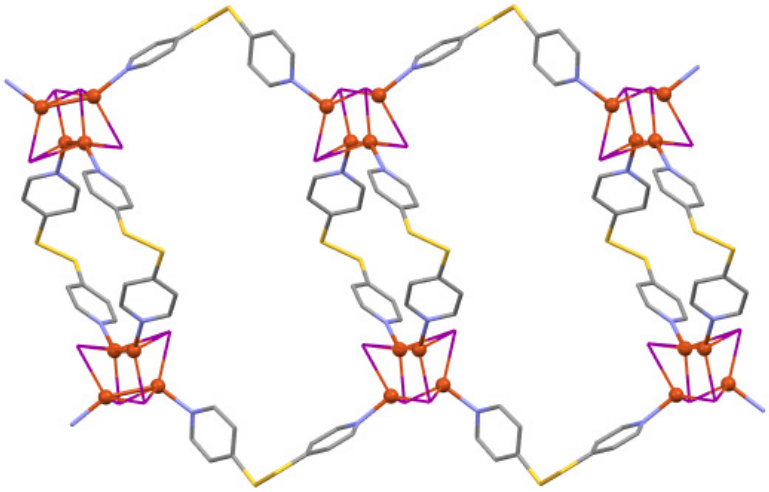

(b)

3.8. Miscellaneous Coordination Polymers

This section covers **dtdp**-based coordination polymers that do not fit into one of the categories in the previous sections. These compounds are listed in Table 7. All these coordination polymers contain, in addition to **dtdp**, other bridging ligands, which can lead to intricate coordination networks. *In situ* reaction of $Zn(NO_3)_2\cdot 6H_2O$, **dtdp**, phthalic acid and sodium hydroxide led to colourless crystals of $[Zn\{\mu\text{-}C_6H_4(COO)_2\}(\mu\text{-}\mathbf{dtdp})\cdot H_2O]_n$ (TAWTOC). The compound can be thought of as a one-dimensional repeated rhomboids coordination polymer, in which the nodes comprise two tetrahedrally coordinated Zn(II) ions linked by two μ-phthalato ligands (Figure 31), the two carboxylate groups of which are both monodentate-bound. The Zn(II) ions and **dtdp** ligands form achiral rhomboids (see also Section 3.2), which lie about inversion centres in the crystal. The rhomboids and the macrocylic units generated by Zn(II) and the μ-phthalato ligands thus alternate and are oriented perpendicular to one another in the polymer strands.

Layering a solution of **dtdp** in acetontrile onto a solution of $Zn(NO_3)_2\cdot 6H_2O$, *cis*-1,2-cyclohexanedicarboxylic acid and ammonia in water afforded colourless crystals of $[Zn_2\{\mu\text{-}C_6H_8(COO)_2\}_2(\mu\text{-}\mathbf{dtdp})_2\cdot 4.5H_2O]_n$ (EPEYII) [99]. Figure 32 depicts a section of the complicated *ca.* 22.3 Å thick coordination network that extends periodically in two dimensions. The asymmetric unit contains two Zn(II) ions, two μ-**dtdp** and two μ-*cis*-1,2-cyclohexanedicarboxylate

ligands. One of the two crystallographically distinct *μ*-**dtdp** liagnds is involved in an arched chain-like arrangement with Zn1, while the other forms rhomboids about a centre of symmetry with Zn2. The *μ*-*cis*-1,2-cyclohexanedicarboxylate ligands link Zn1 and Zn2. The cyclohexane rings adopt the chair conformation and each bears a carboxylate group in equatorial and axial positions. All four distinct carboxylate groups are asymmetrically bidentate-bound to the Zn(II) ions. Both Zn1 and Zn2 are hexa-coordinated with a severe distortion from the regular octahedral geometry as a consequence of the chelate angle of the carboxylate groups.

Table 7. Selected structural parameters for miscellaneous **dtdp**-based coordination polymers that contain additional organic bridging ligands other than **dtdp**.

Compound	C–S–S–C torsion angle (°)	M···M separation (Å) [a]	Reference	CSD Refcode
$[Zn\{\mu\text{-}C_6H_4(COO)_2\}(\mu\text{-dtdp})\cdot H_2O]_n$ [b]	80.1	9.76	[49]	TAWTOC
$[Zn_2\{\mu\text{-}C_6H_8(COO)_2\}_2(\mu\text{-dtdp})_2\cdot 4.5H_2O]_n$ [c]	−82.0, 80.4	10.39, 10.05	[99]	EPEYII
$[Zn(\mu\text{-}C_4H_2O_4)(\mu\text{-dtdp})]_n$ [d]	98.5	11.52	[69]	BOKXOP
$[Mn\{\mu\text{-}C_6H_4(COO)_2\}(\mu\text{-dtdp})\cdot dtdp]_n$ [e]	92.6	11.43	[100]	LAZCUL
$[Eu(\mu_3\text{-}C_4H_4O_5)(\mu\text{-}C_4H_4O_5)_2\{Ni(\mu\text{-dtdp})\}_2\cdot 11\ H_2O]_n$ [f]	92.7	10.78	[101]	OTUFUF
$[Co(\mu\text{-dca})_2(\mu\text{-dtdp})]_n$ [g]	65.9	7.30	[102]	XEGHFOH
$[\{Cu(\mu\text{-}C_7H_3NO_4)(H_2O)\}_2(\mu\text{-dtdp})\cdot CH_3OH\cdot 3\ H_2O]_n$ [h]	89.5	10.58	[103]	IMOTAG
$[\{Cu(\mu\text{-}C_2H_6NO)(\mu\text{-dtdp})\}CF_3SO_3\cdot CH_3OH]_n$ [i]	87.5	10.55	[104]	NOCJUL
$[\{Cu(\mu\text{-}C_3H_8NO)(\mu\text{-dtdp})\}BF_4]_n$ [j]	88.0	10.59	[104]	NOCKAS

[a] Refers to the M···M separation through the **dtdp** ligand; [b] $C_6H_4(COO)_2^{2-}$ = phthalate; [c] $C_6H_8(COO)_2^{2-}$ = 1,2-cyclohexanedicarboxylate; [d] $C_4H_2O_4^{2-}$ = fumarate; [e] $C_6H_4(COO)_2^{2-}$ = terephthalate; [f] $C_4H_4O_5^{2-}$ = oxydiacetate; [g] dca^- = dicyanamide; [h] $C_7H_3NO_4^{2-}$ = pyridine-2,5-dicarboxylate; [i] $C_2H_6NO^-$ = 2-aminoethanolate; [j] $C_3H_8NO^-$ = 3-aminopropanolate.

Figure 31. Coordination polymer strand in $[Zn\{\mu\text{-}C_6H_4(COO)_2\}(\mu\text{-dtdp})\cdot H_2O]_n$ (TAWTOC).

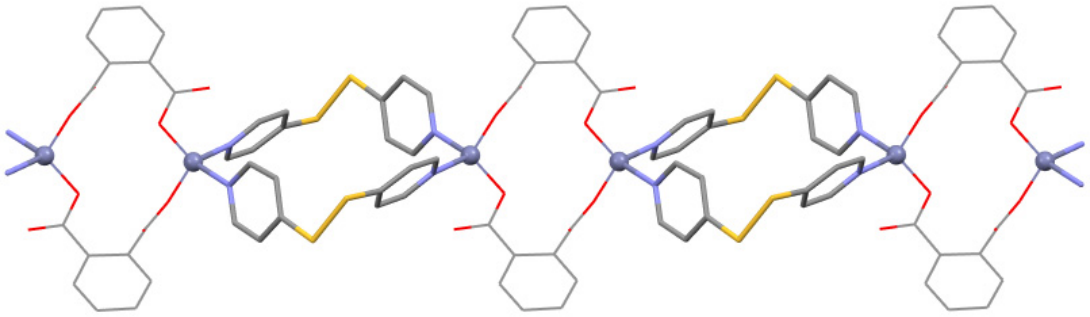

Figure 32. Section of the coordination network in $[Zn_2\{\mu\text{-}C_6H_8(COO)_2\}_2(\mu\text{-}\mathbf{dtdp})_2\cdot 4.5H_2O]_n$ (EPEYII), viewed perpendicular to the slab.

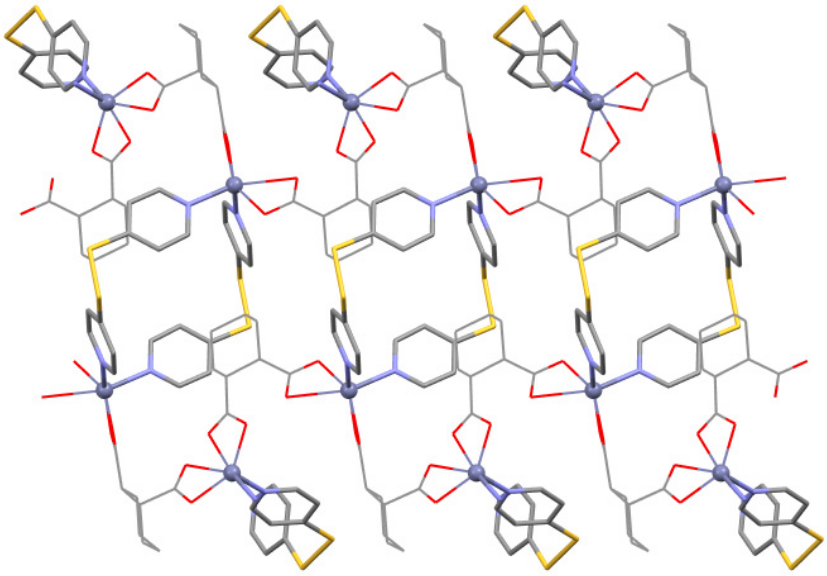

Reaction of $Zn(NO_3)_2\cdot 6H_2O$ and fumaric acid in methanol gave colourless blocks of the neutral two-dimensional coordination network $[Zn(\mu\text{-}C_4H_2O_4)(\mu\text{-}\mathbf{dtdp})]_n$ (BOKXOP, $C_4H_2O_4^{2-}$ = fumarate) [69]. The isomer maleic acid afforded a cationic one-dimensional coordination polymer of the repeated rhomboid type with hydrogen maleate as counter-ions (BOKXIJ, see Section 3.2) under the same conditions. In BOKXOP (Figure 33a), the Zn(II) ions provide tetrahedral nodes, which are joined by **dtdp** ligands to form arched chains (see Section 3.3) in one dimension. In the second dimension, arched chains of opposite chirality are connected through μ-fumarato ligands, whose carboxylato groups are both monodentate bound to Zn(II), completing the tetrahedral coordination sphere. The fumarato-bridged Zn···Zn distance is 9.37 Å. The corrugated (4,4) net layers so formed are twofold interpenetrated in the crystal. $[Mn\{\mu\text{-}C_6H_4(COO)_2\}(\mu\text{-}\mathbf{dtdp})\cdot\mathbf{dtdp}]_n$ (LAZCUL) [100] is topologically similar to BOKXIJ. However, arched chains of the same handedness are linked into (4,4) net sheets by μ-terephthalato ligands (Figure 33b). The coordination environment of Mn(II) is octahedral; two pyridyl groups of **dtdp** and two aqua ligands each occupy two equatorial *cis* coordination sites. The carboxylate groups of the terephthalato ligands are monodentate-bound in the apical positions. The **dtdp**- and terephthalato-bridged Mn···Mn distances are equal by symmetry. In the crystal, two (4,4) net sheets of the same handedness are interpenetrated, but the crystal structure is centrosymmetric, so both enantiomers are present. Temperature-dependent magnetic susceptibility measurements revealed very weak antiferromagnetic coupling in LAZCUL. $[Eu(\mu_3\text{-}C_4H_4O_5)(\mu\text{-}C_4H_4O_5)_2\{Ni(\mu\text{-}\mathbf{dtdp})\}_2\cdot 11H_2O]_n$ (OTUFUF) represents a unique example of a **dtdp**-based heterobimetallic coordination network [101]. Green block-shaped crystals of OTUFUF were obtained by reaction of 2,2′-oxydiacetic acid, **dtdp**, $Ni(NO_3)_2\cdot 6H_2O$ and Eu_2O_3 in aqueous solution at 80 °C at a pH of 5.0. Figure 34 shows a section of the intricate two-dimensional coordination network in OTUFUF. There are essentially two fundamental structural units, that is, arched chains (see Section 3.3) of the composition $[cis\text{-}Ni(H_2O)_2(\mu\text{-}\mathbf{dtdp})]_n^{n2+}$ and homoleptic tris-chelate europium(III) complexes of 2,2′-oxydiacetate. The coordination number of Eu(III) is nine and the coordination sphere is best described as a distorted trigonal tricapped prism. Layers of $[cis\text{-}Ni(H_2O)_2(\mu\text{-}\mathbf{dtdp})]_n^{n2+}$ arched chains of the same chirality diagonally cross one another,

extending in the [011] and [0 $\bar{1}$ 1] directions of the orthorhombic unit cell (space group *Fdd*2). The Eu(III) ions in each layer are thus captured in a chiral environment. Although each layer contains **dtdp** ligands of exclusively *P* or *M* conformation, the crystal structure contains both in alternate layers. The [*cis*-Ni(H_2O)$_2$(μ-**dtdp**)]$_n^{n2+}$ strands are interlinked by the tris(2,2′-oxydiacetato)europium(III) building blocks via the peripheral carboxylato oxygen atoms of the chelate ligands. These complete the octahedral coordination environment of Ni(II). The tris(2,2′-oxydiacetato)europium(III) complexes themselves can therefore be regarded as metalloligands. However, on closer inspection, the 2,2′-oxyacetato ligands act differently with their peripheral carboxylato oxygen atoms. One bridges two Ni(II) ions via both carboxylato groups and thus exhibts an overall μ_3-bridging mode, while the remaining two are each bonded solely to one Ni(II) ion. Thus, each tris(2,2′-oxydiacetato)-europium(III) building block connects four Ni(II) ions.

Figure 33. Two-dimensional coordination networks with (4,4) net topology in (**a**) [Zn(μ-$C_4H_2O_4$)(μ-**dtdp**)]$_n$ (BOKXOP) and (**b**) [Mn{μ-C_6H_4(COO)$_2$}(μ-**dtdp**)·**dtdp**]$_n$ (LAZCUL).

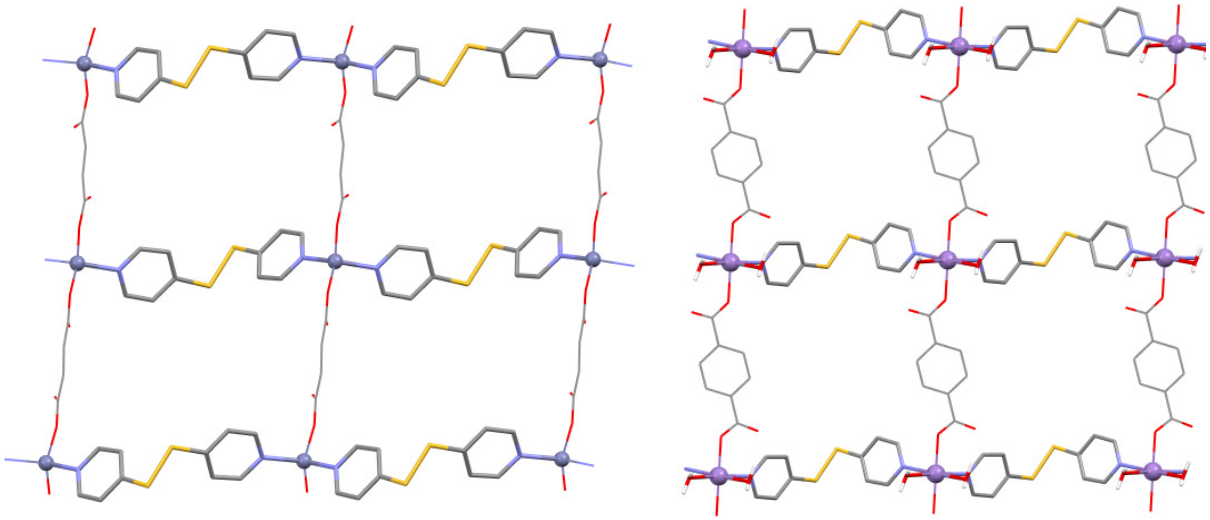

(a) **(b)**

Figure 34. Section of the two-dimensional coordination network in [Eu(μ_3-$C_4H_4O_5$)(μ-$C_4H_4O_5$)$_2${Ni(μ-**dtdp**)}$_2$·11H_2O]$_n$ (OTUFUF), viewed approximately along the [010] direction.

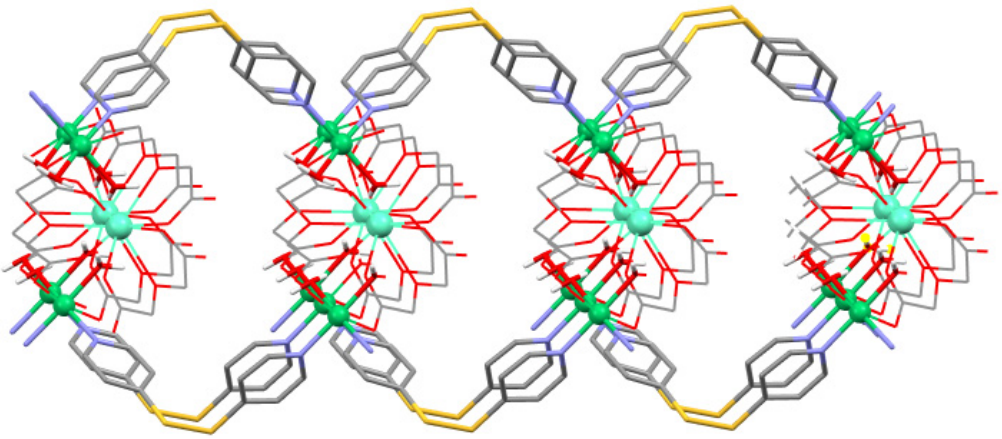

$[Co(\mu\text{-dca})_2(\mu\text{-}\mathbf{dtdp})]_n$ (XEGHOH) was obtained by reaction of $Co(NO_3)_2{\cdot}6H_2O$, **dtdp** and sodium dicyanamide (dca) in a methanol/water mixture [102]. XEGHOH represents a triply linked one-dimensional coordination polymer (Figure 35). The underlying topology is a zigzag chain (see Section 3.4) composed of alternately arranged Co(II) ions and μ-**dtdp** ligands. However, the Co(II) ions are additionally linked by two dicyanamido ligands. The observed triple linkage leads to a remarkably short intrachain Co···Co distance and an exceptionally small C–S–S–C torsion angle for **dtdp** (Table 7), which indicates strain in the macrocyclic entities. In crystal, the octahedrally coordinated Co(II) ions are located on inversion centres and a crystallographic twofold rotation axis runs through the disulfide moiety of **dtdp**. Weak antiferromagnetic coupling in XEGHOH has been mentioned.

Figure 35. Coordination polymer strand in $[Co(\mu\text{-dca})_2(\mu\text{-}\mathbf{dtdp})]_n$ (XEGHOH).

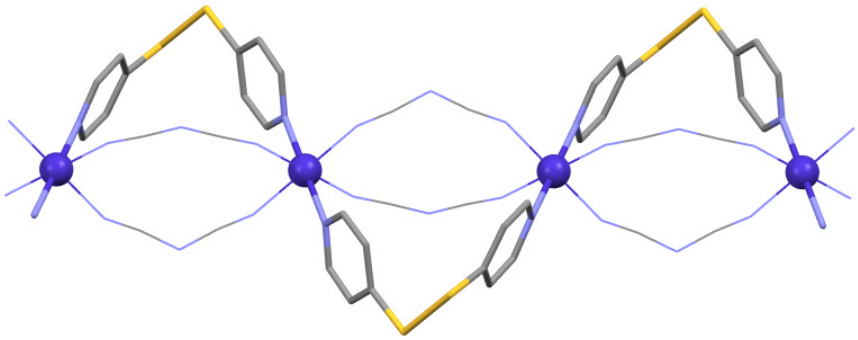

$[\{Cu(\mu\text{-}C_7H_3NO_4)(H_2O)\}_2(\mu\text{-}\mathbf{dtdp})\cdot CH_3OH\cdot 3H_2O]_n$ (IMOTAG, $C_7H_3NO_4^{2-}$ = pyridine-2,6-dicarboxylate) is another example of a two-dimensional coordination network with a layer structure (Figure 36) [103]. Pyridine-2,5-dicarboxylato ligands join Cu(II) ions to form helices along 2_1 screw axes parallel to the [010] direction (space group $P2_1/n$). There are two crystallographically distinct $[Cu(\mu\text{-}C_7H_3NO_4)(H_2O)]_n$ helices in the structure, which are alternately interlinked by **dtdp**. Both Cu1 and Cu2 exhibit a square-pyramidal coordination sphere. The pyridyl group and the carboxylate group in the 2-position of the pyridine-2,5-dicarboxylato ligand form a five-membered chelate ring in the basal plane. The remaining two *cis* coordination sites in the basal plane are occupied by a monodentate-bound carboxylate group in the 5-position of the pyridine-2,5-dicarboxylato ligand of an adjacent unit in a helix and a pyridyl group of **dtdp**. An aqua ligand fills the apical position. It is interesting to note that the $[Cu(\mu\text{-}C_7H_3NO_4)(H_2O)]_n$ helices and the **dtdp** ligands that link them into two-dimensional sheets exhibit the same handedness. In the crystal, sheets of opposite chirality stack in an alternating fashion.

In $[\{Cu(\mu\text{-}C_2H_6NO)(\mu\text{-}\mathbf{dtdp})\}CF_3SO_3\cdot CH_3OH]_n$ (NOCJUL, $C_2H_6NO^-$ = 2-aminoethanolate) and $[\{Cu(\mu\text{-}C_3H_8NO)(\mu\text{-}\mathbf{dtdp})\}BF_4]_n$ (NOCKAS, $C_3H_8NO^-$ = 3-aminopropanolate), alkoxido-bridged copper(II) dimers are linked into two-dimensional coordination networks by **dtdp** [104]. Figure 37a shows the coordination network in NOCJUL, which is exemplary for both topologically similar structures. Centrosymmetric $Cu_2(\mu\text{-}C_2H_6NO)_2^{2+}$ and $Cu_2(\mu\text{-}C_3H_8NO)_2^{2+}$ entities with central Cu_2O_2 four-membered rings serve as nodes in NOCJUL and NOCKAS, respectively. The Cu(II) ions are penta-coordinated with a square-pyramidal coordination sphere. The 2-aminoethanolato and the 3-aminopropanolato ligands respectively form five- and six-membered chelate rings, thereby occupying two *cis* coordination sites of the Cu(II) ions in the basal plane. Another *cis* coordination site is filled by the bridging

alkoxido oxygen atom. The remaining basal *cis* site and the apical position are occupied by pyridyl groups of **dtdp**. Each dinuclear metal node is connected to four adjacent nodes in the network. Thus, the structures can be topologically regarded as (4,4) nets. It is noteworthy that the coordination networks in NOCJUL and NOCKAS are almost superimposable (Figure 37b), even though the non-coordinating anions in the two structures are different ($CF_3SO_3^-$ and BF_4^-, respectively) and NOCJUL contains in addition one methanol molecule per formula unit.

Figure 36. Two-dimensional coordination network in $[\{Cu(\mu\text{-}C_7H_3NO_4)(H_2O)\}_2(\mu\text{-}\mathbf{dtdp})\cdot CH_3OH\cdot 3H_2O]_n$ (IMOTAG).

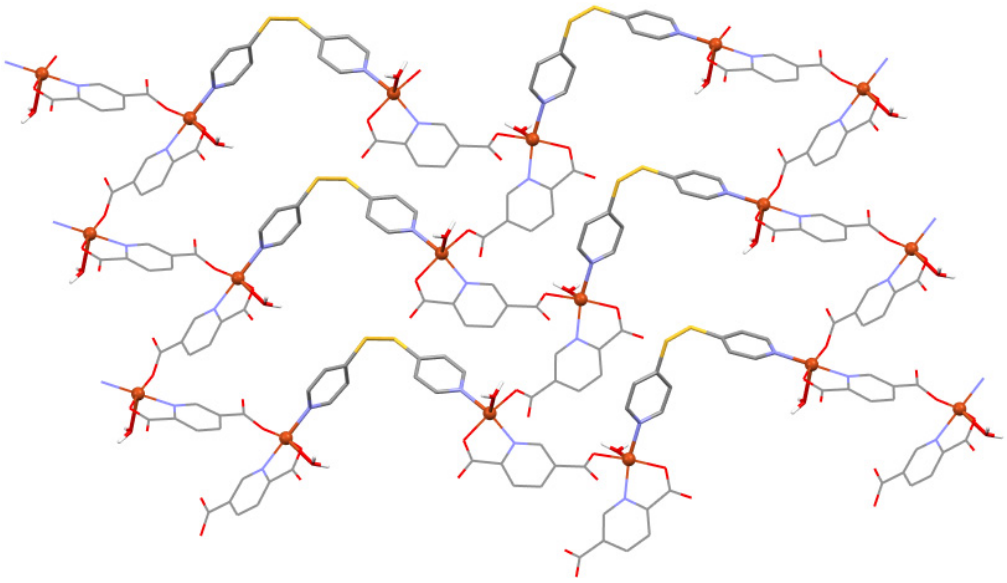

Figure 37. (**a**) Two-dimensional coordination network in $[\{Cu(\mu\text{-}C_2H_6NO)(\mu\text{-}\mathbf{dtdp})\}CF_3SO_3\cdot CH_3OH]_n$ (NOCJUL); (**b**) Superposition of the coordination networks of NOCJUL (red) and NOCKAS (black).

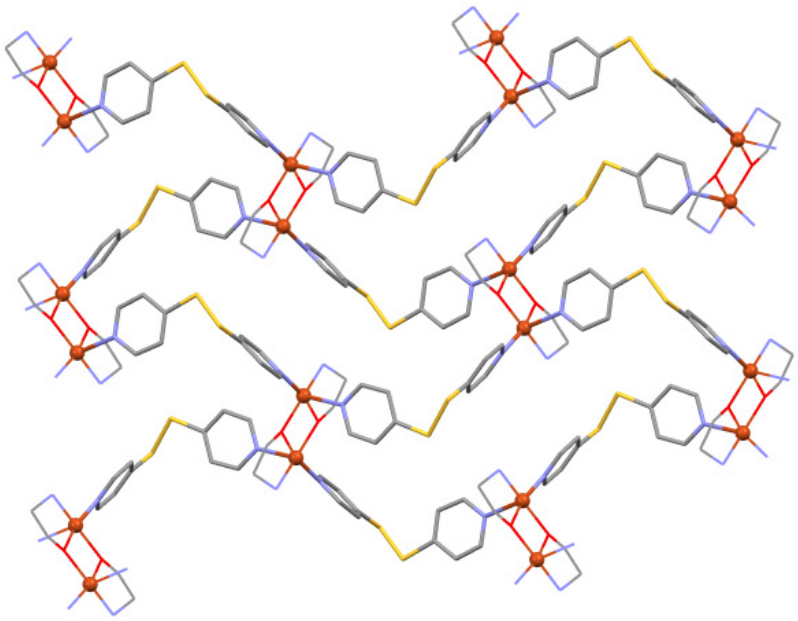

(a)

Figure 37. *Cont.*

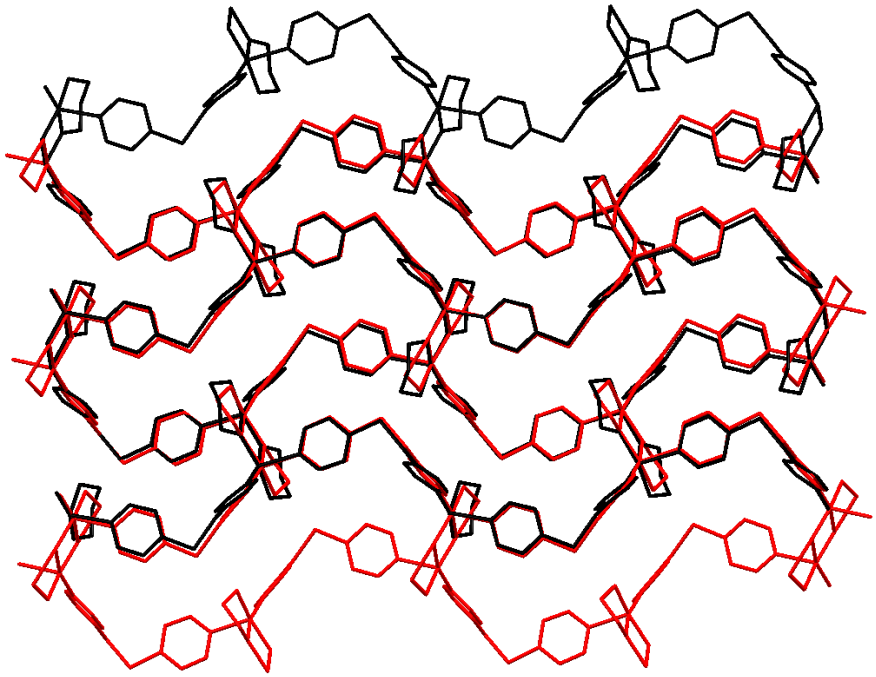

(b)

4. Conclusions

The results reviewed in this contribution illustrate the versatility of the **dtdp** bent bridging ligand in the generation of metallosupramolecular assemblies with various dimensionalities and structures. M_2L_2 macrocycles represent the sole type of discrete metallosupramolecular compounds that have been obtained from **dtdp** by solution self-assembly or crystal engineering strategies. We are not aware of metallosupramolecular box or cage compounds derived from this ligand. In contrast, there is a rich structural chemistry of **dtdp**-based coordination polymers. Those with periodicity in one-dimension represent the majority of the structures reported. Two-dimensional coordination polymers propagated exclusively by **dtdp** are scarce, and three-dimensional ones that fulfil this criterion have not been described to our knowledge. The formation of such a structure seems sterically unfavourable owing to characteristic angular nature of **dtdp**. Although the **dtdp** molecule exhibts axial chirality, there are only two crystal structures that contain exclusively one conformational enantiomer (GUXPIZ and KEXDIB). Bearing in mind that the rotational barrier between the *P* and *M* forms of **dtdp** is low in solution and that 5%–10% of all racemic compounds are known to crystallise as conglomerates, the intrinsic axial chirality of **dtdp** may not be the determining factor in the formation of these two structures. In contrast, chiral M_2L_2 macrocycles, coordination polymer strands or networks are found together with their enantiomers in many crystal structures. As far as we can ascertain, a systematic crystal engineering study on metallosupramolecular compounds involving **dtdp** and chiral, enantiopure resolving agents, for example chiral co-ligands at the metal ions or chiral guest molecules, has not been reported so far.

Acknowledgments

We would particularly like to thank William S. Sheldrick for his generous support and Christina Dietz for her contributions to our own work cited in this review. We would also like to thank the two anonymous reviewers for useful suggestions. Financial support from Bayer MaterialScience is gratefully acknowledged.

Conflict of Interest

The authors declare no conflict of interest.

References

1. Constable, E.C. Higher oligopyridines as a structural motif in metallosupramolecular chemistry. *Prog. Inorg. Chem.* **1994**, *42*, 67–138.
2. Steel, P.J. Metallosupramolecular chemistry; what is it? *Chem. N. Z.* **2003**, *67*, 57–60.
3. Cook, T.R.; Zheng, Y.-R.; Stang, P.J. Metal-organic frameworks and self-assembled supramolecular coordination complexes: Comparing and contrasting the design, synthesis, and functionality of metal-organic materials. *Chem. Rev.* **2013**, *113*, 734–777.
4. Batten, S.R.; Champness, N.R.; Chen, X.M.; Garcia-Martinez, J.; Kitagawa, S.; Öhrström, L.; O'Keeffe, M.; Suh, M.P.; Reedijk, J. Coordination polymers, metal-organic frameworks and the need for terminology guidelines. *CrystEngComm* **2012**, *14*, 3001–3004.
5. Fujita, M.; Yoshizawa, M. New Properties and Reactions in Self-Assembled Coordination M_6L_4 Cages. In *Modern Supramolecular Chemistry*; Diederich, F., Stang, P.J., Tykwinski, R.R., Eds.; Wiley-VCH: Weinheim, Germany, 2008.
6. Alexeev, Y.E.; Kharisov, B.; Hernández García, T.H.; Garnovskii, A. Coordination motifs in modern supramolecular chemistry. *Coord. Chem. Rev.* **2010**, *254*, 794–831.
7. De, S.; Mahata, K.; Schmittel, M. Metal-coordination-driven dynamic heteroleptic architectures. *Chem. Soc. Rev.* **2010**, *39*, 1555–1575.
8. Wiester, M.J.; Ulmann, P.A.; Mirkin, C.A. Enzyme mimics based upon supramolecular coordination chemistry. *Angew. Chem. Int. Ed.* **2011**, *50*, 114–137.
9. Debata, N.B.; Tripathy, D.; Chand, D.K. Self-assembled coordination complexes from various palladium(II) components and bidentate or polydentate ligands. *Coord. Chem. Rev.* **2012**, *256*, 1831–1945.
10. Stang, P.J. Abiological self-assembly via coordination: Formation of 2D metallacycles and 3D metallacages with well-defined shapes and sizes and their chemistry. *J. Am. Chem. Soc.* **2012**, *134*, 11829–11830.
11. Kuppler, R.J.; Timmons, D.J.; Fang, Q.R.; Lia, J.R.; Makala, T.A.; Young, M.D.; Yuan, D.; Zhao, D.; Zhuang, W.; Zhou, H.C. Potential applications of metal-organic frameworks. *Coord. Chem. Rev.* **2009**, *253*, 3042–3066.
12. Lee, J.; Farha, O.K.; Roberts, J.; Scheidt, K.A.; Nguyen, S.T.; Hupp, J.T. Metal-organic framework materials as catalysts. *Chem. Soc. Rev.* **2009**, *38*, 1450–1459.

13. Farrusseng, D.; Aguado, S.; Pinel, C. Metal-organic frameworks: Opportunities for catalysis. *Angew. Chem. Int. Ed.* **2009**, *48*, 7502–7513.
14. Shimomura, S.; Bureekaew, S.; Kitagawa, S. Porous coordination polymers towards gas technology. *Struct. Bond.* **2009**, *132*, 51–86.
15. Horike, S.; Shimomura, S.; Kitagawa, S. Soft porous crystals. *Nat. Chem.* **2009**, *1*, 695–704.
16. Janiak, C.; Vieth, J.K. MOFs, MILs and more: Concepts, properties and applications for porous coordination networks (PCNs). *New J. Chem.* **2010**, *34*, 2366–2388.
17. Morozan, A.; Jaouen, F. Metal organic frameworks for electrochemical applications. *Energy Environ. Sci.* **2012**, *5*, 9269–9290.
18. Holliday, B.J.; Mirkin, C.A. Strategies for the construction of supramolecular compounds through coordination chemistry. *Angew. Chem. Int. Ed.* **2001**, *40*, 2022–2043.
19. Robson, R. A net-based approach to coordination polymers. *J. Chem. Soc. Dalton Trans.* **2000**, 3735–3744.
20. Moss, G.P. Basic terminology of stereochemistry (IUPAC Recommendations 1996). *Pure Appl. Chem.* **1996**, *68*, 2193–2222.
21. Kessler, H.; Rundel, W. Nachweis innermolekularer beweglichkeit durch NMR-spektroskopie, VI. Konformation und gehinderte rotation in disulfiden und diseleniden. *Chem. Ber.* **1968**, *101*, 3350–3357.
22. Zhu, H.B.; Gou, S.H. *In situ* construction of metal-organic sulfur-containing heterocycle frameworks. *Coord. Chem. Rev.* **2011**, *255*, 318–338.
23. Dietz, C.; Seidel, R.W.; Oppel, I.M. Crystal structure of *catena*-(μ_2-sulfato)-diaqua-(1,10-phenanthroline)-cobalt(II), $Co(H_2O)_2(C_{12}H_2N_2)SO_4$ at 106 K and refinement of crystal structure of *catena*-(μ_2-sulfato)-diaqua-(1,10-phenanthroline)copper(II), $Cu(H_2O)_2(C1_2H_2N_2)SO_4$ at 106 K. *Z. Krist. New Cryst. Struct.* **2009**, *224*, 509–511.
24. Horikoshi, R.; Mochida, T. Metal complexes of 4,4′-dipyridyldisulfide—Structural diversity derived from a twisted ligand with axial chirality. *Coord. Chem. Rev.* **2006**, *250*, 2595–2609.
25. Ghosh, A.K.; Ghoshal, D.; Lu, T.H.; Mostafa, G.; Chaudhuri, N.R. Novel solid-state molecular self-assemblies of manganese (II) constructed with flexible ligands: Influences of π–π and C–H···π interactions on their crystal packing. *Cryst. Growth Des.* **2004**, *4*, 851–857.
26. Carballo, R.; Covelo, B.; Fernández-Hermida, N.; García-Martinez, E.; Lago, A.B.; Vázquez-López, E.M. Structural versatility in copper(II) α-hydroxycarboxylate complexes with the twisted ligands 4,4′-dipyridyldisulfide and bis(4-pyridylthio)methane: From molecular compounds to two-dimensional coordination polymers. *Cryst. Growth Des.* **2008**, *8*, 995–1004.
27. Carballo, R.; Covelo, B.; Fernández-Hermida, N.; Lago, A.B.; Vázquez-López, E.M. Structural evidence for metalloaromaticity in a new molecular complex with the divergent ligand 4,4′-dipyridyldisulfide. *J. Mol. Struct.* **2009**, *936*, 87–91.
28. Seidel, R.W.; Dietz, C.; Oppel, I.M. A polymeric arched chain and a chair-like M_2L_2-metallamacrocycle c*rystal engineered* of $[M(phen)]^{2+}$ (M = Cu, Cd; phen = 1,10-Phenanthroline) corner units and the bent ligand 4,4′-dithiodipyridine. *Z. Anorg. Allg. Chem.* **2011**, *637*, 94–101.
29. Wang, H.; Guo, X.Q.; Zhong, R.; Hou, X.F. Reactions of half-sandwich Co(III) complexes with heterocyclic thione ligands: η^2-N, S coordination mode and formation of S–S bond. *J. Organomet. Chem.* **2009**, *694*, 1567–1570.

30. Coe, B.J.; Hayat, S.; Beddoes, R.L.; Helliwell, M.; Jeffery, J.C.; Batten, S.R.; White, P.S. Synthesis and properties of ligand-bridged dinuclear complexes containing *trans*-bis [*o*-phenylenebis(dimethylarsine)]chlororuthenium(II) centres. *J. Chem. Soc. Dalton Trans.* **1997**, 591–600.
31. Han, Y.F.; Li, H.; Fei, Y.; Lin, Y.J.; Zhang, W.Z.; Jin, G.X. Synthesis and structural characterization of binuclear half-sandwich iridium, rhodium and ruthenium complexes containing 4,4′-dipyridyldisulfide (4DPDS) ligands. *Dalton Trans.* **2010**, *39*, 7119–7124.
32. Allen, F.H. The cambridge structural database: A quarter of a million crystal structures and rising. *Acta Crystallogr. B* **2002**, *B58*, 380–388.
33. Groom, C.R.; Allen, F.H. The cambridge structural database: Experimental three-dimensional information on small molecules is a vital resource for interdisciplinary research and learning. *Wiley Interdiscip. Rev. Comput. Mol. Sci.* **2011**, *1*, 368–376.
34. Thomas, I.R.; Bruno, I.J.; Cole, J.C.; Macrae, C.F.; Pidcock, E.; Wood, P.A. WebCSD: The online portal to the cambridge structural database. *J. Appl. Cryst.* **2010**, *43*, 362–366.
35. Macrae, C.F.; Edgington, P.R.; McCabe, P.; Pidcock, E.; Shields, G.P.; Taylor, R.; Towler, M.; van de Streek, J. Mercury: Visualization and analysis of crystal structures. *J. Appl. Cryst.* **2006**, *39*, 453–457.
36. Macrae, C.F.; Bruno, I.J.; Chisholm, J.A.; Edgington, P.R.; McCabe, P.; Pidcock, E.; Rodriguez-Monge, L.; Taylor, R.; van de Streek, J.; Wood, P.A. Mercury CSD 2.0—New features for the visualization and investigation of crystal structures. *J. Appl. Cryst.* **2008**, *41*, 466–470.
37. Li, C.P.; Du, M. Role of solvents in coordination supramolecular systems. *Chem. Commun.* **2011**, *47*, 5958–5972.
38. Batten, S.R.; Champness, N.R.; Chen, X.M.; Garcia-Martinez, J.; Kitagawa, S.; Öhrström, L.; O'Keeffe, M.; Suh, M.P.; Reedijk, J. Terminology of metal-organic frameworks and coordination polymers (IUPAC Provisional Recommendation), 2013. Available online: http://www.iupac.org/home/publications/provisional-recommendations/under-review-by-the-authors/under-review-by-the-authors-container/terminology-of-metal-organic-frameworks-and-coordination-polymers.html (accessed on 10 May 2013).
39. Moulton, B.; Zaworotko, M.J. From molecules to crystal engineering: Supramolecular isomerism and polymorphism in network solids. *Chem. Rev.* **2001**, *101*, 1629–1658.
40. Zhang, J.P.; Huang, X.C.; Chen, X.M. Supramolecular isomerism in coordination polymers. *Chem. Soc. Rev.* **2009**, *38*, 2385–2396.
41. Desiraju, G.R.; Vittal, J.J.; Ramanan, A. *Crystal Engineering: A Textbook*; World Scientific: Singapore, 2011.
42. Wells, A.F. *Three-Dimensional Nets and Polyhedra*; Wiley: New York, NY, USA, 1977.
43. Wells, A.F. *Structural Inorganic Chemistry*; Oxford University Press: Oxford, UK, 1984.
44. Desiraju, G.R. Crystal engineering: A holistic view. *Angew. Chem. Int. Ed.* **2007**, *46*, 8342–8356.
45. Tabellion, F.M.; Seidel, S.R.; Arif, A.M.; Stang, P.J. Discrete supramolecular architecture *vs.* crystal engineering: The rational design of a platinum-based bimetallic assembly with a chairlike structure and its infinite, copper analogue. *J. Am. Chem. Soc.* **2001**, *123*, 7740–7741.
46. Xiao, X.Q.; Jia, A.Q.; Lin, Y.J.; Jin, G.X. Self-assembly of palladium-based macrocycles with *N*-heterocyclic carbene as the "corner" ligand. *Organometallics* **2010**, *29*, 4842–4848.

47. Yu, X.Y.; Maekawa, M.; Morita, T.; Chang, H.C.; Kitagawa, S.; Jin, G.X. Solvent-dependent formation of di- and trinuclear rhodium and iridium complexes bridged by *N*,*N*′-donor ligands. *Bull. Chem. Soc. Jpn.* **2002**, *75*, 267–275.
48. Horikoshi, R.; Mochida, T.; Kurihara, M.; Mikuriya, M. Supramolecular isomerism in self-assembled complexes from 4,4′-dipyridyl disulfide and $M(hfac)_2$: Coordination polymers (M = Mn) and metallamacrocycles (M = Co, Ni). *Cryst. Growth Des.* **2005**, *5*, 243–249.
49. Zhu, H.L.; Lin, J.L.; Xu, W.; Zhang, J.; Zheng, Y.Q. Self-assembly of new Zn(II) supramolecular complexes from 4,4′-dipyridyldisulfide. *J. Coord. Chem.* **2011**, *64*, 2088–2100.
50. Horikoshi, R.; Mochida, T.; Moriyama, H. Coordination polymers from $M(hfac)_2$ [M = Cu^{II}, Mn^{II}] and 4,4′-Dipyridyldisulfide. *Inorg. Chem.* **2001**, *40*, 2430–2433.
51. Kondo, M.; Shimamura, M.; Noro, S.-I.; Kimura, Y.; Uemura, K.; Kitagawa, S. Synthesis and structures of coordination polymers with 4,4′-dipyridyldisulfide. *J. Solid State Chem.* **2000**, *152*, 113–119.
52. Yan, L. Crystal structure of diaqua-bis(4,4′-dipyridyldisulfide)cadmium(II) dinitrate–methanol–water (1:2:2), $[Cd(C_{10}H_8N_2S_2)_2(H_2O)_2][NO_3]_2{\cdot}2CH_3OH{\cdot}2H_2O$. *Z. Kristallogr. New Cryst. Struct.* **2008**, *223*, 533–534.
53. Horikoshi, R.; Mikuriya, M. Self-assembly of repeated rhomboidal coordination polymers from 4,4′-dipyridyl disulfide and ZnX_2 salts (X = SCN, NO_3, ClO_4). *Cryst. Growth Des.* **2005**, *5*, 223–230.
54. Seidel, R.W.; Dietz, C.; Oppel, I.M. Structural insight into repeated-rhomboid coordination polymers from 4,4′-dithiodipyridine and zinc nitrate. *Struct. Chem.* **2011**, *22*, 1225–1232.
55. Ghosh, A.K.; Ghoshal, D.; Ribas, J.; Zangrando, E.; Chaudhuri, N.R. Higher dimensional networks of Mn(II) azide/cyanate using flexible N-donor ligands: Synthesis, crystal structure and magnetic properties. *J. Mol. Struct.* **2006**, *796*, 195–202.
56. Hwang, I.H.; Jo, Y.D.; Kim, H.Y.; Kang, J.; Noh, J.Y.; Hyun, M.Y.; Kim, C.; Kim, Y.; Kim, S.J. Novel Mn^{II} coordination compounds constructed from benzoate and various bipyridyl ligands: Magnetic property and catalytic activity. *Polyhedron* **2012**, *42*, 282–290.
57. de la Pinta, N.; Fidalgo, L.; Madariaga, G.; Lezama, L.; Cortés, R. Guest driven structural correlations in DPDS [Di(4-pyridyl)disulfide]-based coordination polymers. *Cryst. Growth Des.* **2012**, *12*, 5069–5078.
58. Suen, M.C.; Wang, Y.H.; Hsu, Y.F.; Yeh, C.W.; Chen, J.D.; Wang, J.C. Syntheses and structural characterization of transition metal(II) coordination polymers containing 4,4′-dipyridyldisulfide. *Polyhedron* **2005**, *24*, 2913–2920.
59. de la Pinta, N.; Madariaga, G.; Ezpeleta, T.; Fidalgo, M.L.; Lezama, L.; Cortés, R. Spin canting in the $[Co_2(NCO)_4(DPDS)_4]{\cdot}3H_2O$ [DPDS = di(4-pyridyl)disulfide] coordination polymer. *Polyhedron* **2013**, *52*, 1256–1261.
60. Carballo, R.; Covelo, B.; Fernández-Hermida, N.; Vázquez-López, E.M. Synthesis and structures of two one-dimensional coordination polymers: $[Co(NCS)_2(dpds)_2]$ and $[Cu(ox)(Im)_2]$. *Z. Anorg. Allg. Chem.* **2007**, *633*, 1787–1790.
61. Luo, J.; Hong, M.; Wang, R.; Yuan, D.; Cao, R.; Han, L.; Xu, Y.; Lin, Z. Self-assembly of three Cd^{II}- and Cu^{II}-containing coordination polymers from 4,4′-dipyridyl disulfide. *Eur. J. Inorg. Chem.* **2003**, 3623–3632.

62. Manna, S.C.; Konar, S.; Zangrando, E.; Drew, M.G.B.; Ribas, J.; Chaudhuri, N.R. Two new μ-(1,3-Azido)-bridged polymers: Alternating single and double bridges in a 1D Nickel(II) complex and uniform bridge in a 2D copper(II) complex: Syntheses, single-crystal structures and magnetic studies. *Eur. J. Inorg. Chem.* **2005**, 1751–1758.
63. Manna, S.C.; Ribas, J.; Zangrando, E.; Chaudhuri, N.R. Dipyridyl bridged coordination polymers of Cu(II): Synthesis, crystal structure and magnetic study. *Polyhedron* **2007**, *26*, 4923–4928.
64. Carballo, R.; Covelo, B.; Fernández-Hermida, N.; Lago, A.B.; Vázquez-López, E.M. From copper(II) carboxylate to copper(II) 4-pyridylsulfonate coordination polymers as a consequence of the copper(II)-assisted oxidative cleavage of the 4,4′-dipyridyldisulfide ligand. *CrystEngComm* **2009**, *11*, 817–826.
65. Zhu, H.L.; Zhang, J.; Lin, J.L. *catena*-Poly[[[diaquacopper(II)]-bis(μ_2-di-4-pyridyl disulfide-$\kappa^2N:N'$)] bis(hydrogen phthalate) monohydrate]. *Acta Cryst.* **2010**, *E66*, m185.
66. Brito, I.; Vallejos, J.; Mundaca, A.; Cardenas, A.; Albanez, J.; Vargas, D.; Lopez-Rodriguez, M. Supramolecular structure, thermal and spectroscopic properties of a new coordination polymer: Catena-bis(μ_2-4,4′-dipyridyldisulfide-κ^2N,N′)-bis(AQUO)-copper(II)di-trifluoro-methanesulfonate. *Mol. Cryst. Liq. Cryst.* **2010**, *521*, 158–167.
67. Carballo, R.; Fernández-Hermida, N.; Lago, A.B.; Rodríguez-Hermida, S.; Vázquez-López, E.M. Supramolecular networks through second-sphere coordination based on 1D metal-4,4′-dipyridyldisulfide coordination polymers and hydrogenfumarate or sulfonate anions. *Polyhedron* **2012**, *31*, 118–127.
68. Suen, M.C.; Wang, J.C. Syntheses and structural characterization of inifinite coordination polymers from bipyridyl ligands and zinc salts. *Struct. Chem.* **2006**, *17*, 315–322.
69. Yang, X.; Li, D.; Fu, F.; Tang, L.; Yang, J.; Wang, L.; Wang, Y. Two disparate 2-fold interpenetrating frameworks constructed from Zn^{II}, 4,4′-dipyridyl disulfide and maleic/fumaric acid. *Z. Anorg. Allg. Chem.* **2008**, *634*, 2634–2638.
70. Zhang, J.; Xu, W. *catena*-Poly[[[(2-phenylacetato-κO)zinc(II)]bis[μ-4,4′-(disulfanediyl)-dipyridine-$\kappa^2N:N'$]] monohydrate]. *Acta Cryst.* **2010**, *E66*, m788–m789.
71. Noro, S.-I. Rational synthesis and characterization of porous Cu(II) coordination polymers. *Phys. Chem. Chem. Phys.* **2010**, *12*, 2519–2531.
72. Long, G.J.; Clarke, P.J. Crystal and Molecular Structures of *trans*-Tetrakis(pyridine)-dichloroiron(II), -nickel(II), and -cobalt(II) and *trans*-Tetrakis(pyridine)dichloroiron(II) monohydrate. *Inorg. Chem.* **1978**, *17*, 1394–1401.
73. Flack, H.D. On enantiomorph-polarity estimation. *Acta Cryst.* **1983**, *A39*, 876–881.
74. Lai, C.S.; Tiekink, E.R.T. Engineering polymers with variable topology—Bipyridine adducts of cadmium dithiophosphates. *CrystEngComm* **2004**, *6*, 593–605.
75. Manna, S.C.; Ghosh, A.K.; Zangrando, E.; Chaudhuri, N.R. 3D supramolecular networks of Co(II)/Fe(II) using the croconate dianion and a bipyridyl spacer: Synthesis, crystal structure and thermal study. *Polyhedron* **2007**, *26*, 1105–1112.
76. Steed, J.W. Should solid-state molecular packing have to obey the rules of crystallographic symmetry? *CrystEngComm* **2003**, *5*, 169–179.
77. Desiraju, G.R. On the presence of multiple molecules in the crystal asymmetric unit ($Z' > 1$). *CrystEngComm* **2007**, *9*, 91–92.

78. Carballo, R.; Covelo, B.; Fernández-Hermida, N.; García-Martínez, E.; Lago, A.B.; Vázquez-López, E.M. Solid state coordination chemistry of copper(II) lactate complexes with the twisted ligands 4,4′-dipyridyldisulfide and bis(4-pyridylthio)methane. *J. Mol. Struct.* **2008**, *892*, 427–432.
79. Seidel, R.W.; Oppel, I.M. *catena*-Poly[[[aqua(ethylenediamine-κ^2N,N')(nitrato-κO)copper(II)]-μ-4,4′-dithiodipyridine-$\kappa^2N:N'$] nitrate monohydrate]. *Acta Cryst.* **2009**, *C65*, m235–m237.
80. Ng, M.T.; Deivaraj, T.C.; Klooster, W.T.; McIntyre, G.J.; Vittal, J.J. Hydrogen-bonded polyrotaxane-like structure containing cyclic $(H_2O)_4$ in $[Zn(OAc)_2(\mu\text{-bpe})]_2{\cdot}H_2O$: X-ray and neutron diffraction studies. *Chem. Eur. J.* **2004**, *10*, 5853–5859.
81. Marsh, R.E. Space groups *P*1 and *Cc*: How are they doing? *Acta Cryst.* **2009**, *B65*, 782–783.
82. Seidel, R.W.; Dietz, C.; Oppel, I.M. Crystal structure of *catena*-[dichlorido-μ_2-4,4′-dithiodipyridine-κ^2N:N'-zinc(II)], $C_{10}H_8Cl_2N_2S_2Zn$. *Z. Kristallogr. New Cryst. Struct.* **2012**, *227*, 305–306.
83. Seidel, R.W.; Dietz, C.; Goddard, R.; Oppel, I.M. Non-merohedrally twinned *catena*-[dibromido-μ-4,4′-dithiodipyridine-κ^2N:N'-zinc(II)]. *J. Chem. Crystallogr.* **2013**, *43*, 229–234.
84. Biradha, K.; Sarkar, M.; Rajput, L. Crystal engineering of coordination polymers using 4,4′-bipyridine as a bond between transition metal atoms. *Chem. Commun.* **2006**, 4169–4179.
85. Seidel, R.W.; Goddard, R.; Zibrowius, B.; Oppel, I.M. A molecular antenna coordination polymer from cadmium(II) and 4,4′-bipyridine featuring three distinct polymer strands in the crystal. *Polymers* **2011**, *3*, 1458–1474.
86. Horikoshi, R.; Mikuriya, M. One-dimensional coordination polymers from the self-assembly of copper(II) carboxylates and 4,4′-dithiobis(pyridine). *Bull. Chem. Soc. Jpn.* **2005**, *78*, 827–834.
87. Aragoni, M.C.; Arca, M.; Crespo, M.; Devillanova, F.A.; Hursthouse, M.B.; Huth, S.L.; Isaia, F.; Lippolis, V.; Verani, G. Predictable and unpredictable reactions between 4,4′-dipyridyldisulfide and phosphonodithioato/dithiophosphato Ni^{II} complexes: Novel coordination polymers and the unique example of 4,4′-dipyridyltrisulfide. *CrystEngComm* **2007**, *9*, 873–878.
88. Chen, D.; Lai, C.S.; Tiekink, E.R.T. Supramolecular aggregation in diimine adducts of zinc(II) dithiophosphates: Controlling the formation of monomeric, dimeric, polymeric (zig-zag and helical), and 2-D motifs. *CrystEngComm* **2006**, *8*, 51–58.
89. Horikoshi, R.; Mochida, T.; Maki, N.; Yamada, S.; Moriyama, H. Coordination polymer complexes of 4,4′-dipyridyldisulfide and AgX ($X = PF_6^-$, ClO_4^-, OTs^-, NO_3^-, BF_4^-) with twisted rhomboid networks, 2-D sheets, and 1-D chain structures. *Dalton Trans.* **2002**, 28–33.
90. Ma, L.F.; Wang, Y.Y.; Wang, L.Y.; Lu, D.H.; Batten, S.R.; Wang, J.G. Two coordination polymers involving triangular and linear trinuclear Co(II) clusters created via *in situ* ligand synthesis. *Cryst. Growth Des.* **2009**, *9*, 2036–2038.
91. O'Keeffe, M.; Peskov, M.A.; Ramsden, S.J.; Yaghi, O.M. The reticular chemistry structure resource (RCSR) database of, and symbols for, crystal nets. *Acc. Chem. Res.* **2008**, *41*, 1782–1789.
92. Delgado, S.; Molina-Ontoria, A.; Medina, M.E.; Pastor, C.J.; Jiménez-Aparicio, R.; Priego, J.L. Structural diversity of copper complexes with angular and linear dipyridyl ligands. *Polyhedron* **2007**, *26*, 2817–2828.
93. Wu, B.L.; Xu, Y.-Q.; Gong, Y.-Q.; Huang, Y.-G.; Hong, M.-C. Linear oxalato- and 4,4′-dipyridyldisulfide-bridged copper(II) coordination polymer involving *in situ* ligand synthesis. *J. Coord. Chem.* **2007**, *60*, 2527–2532.

94. Carballo, R.; Covelo, B.; Fernández-Hermida, N.; García-Martinez, E.; Lago, A.B.; Vázquez, M.; Vázquez-López, E.M. Supramolecular aggregation of hexameric water clusters into a 2D water polymer containing $(H_2O)_{18}$ holes. *Cryst. Growth Des.* **2006**, *6*, 629–631.
95. Ng, M.T.; Deivaraj, T.C.; Vittal, J.J. Self assembly of heptanuclear zinc(II) clusters linked by angular spacer ligands. *Inorg. Chim. Acta* **2003**, *348*, 173–178.
96. Köberl, M.; Cokoja, M.; Herrmann, W.A.; Kühn, F.E. From molecules to materials: Molecular paddle-wheel synthons of macromolecules, cage compounds and metal-organic frameworks. *Dalton Trans.* **2011**, *40*, 6834–6859.
97. Lang, J.P.; Xu, Q.F.; Zhang, W.H.; Li, H.X.; Ren, Z.G.; Chen, J.X.; Zhang, Y. Mo(W)/Cu/S cluster-based supramolecular arrays assembled from preformed clusters $[Et_4N]_4[WS_4Cu_4I_6]$ and $[(n\text{-}Bu)_4N]_2[MoOS_3Cu_3X_3]$ (X = I, SCN) with flexible ditopic ligands. *Inorg. Chem.* **2006**, *45*, 10487–10496.
98. Blake, A.J.; Brooks, N.R.; Champness, N.R.; Crew, M.; Gregory, D.H.; Hubberstey, P.; Schröder, M.; Deveson, A.; Fenske, D.; Hanton, L.R. Topological isomerism in coordination polymers. *Chem. Commun.* **2001**, 1432–1433.
99. Lee, Y.J.; Kim, E.Y.; Kim, S.H.; Jang, S.P.; Lee, T.G.; Kim, C.; Kim, S.J.; Kim, Y. Synthesis, crystal structures, photoluminescence, and catalytic reactivity of novel coordination polymers (0-D, 1-D, 2-D to 3-D) constructed from *cis*-1,2-cyclohexanedicarboxylic acid and various bipyridyl ligands. *New J. Chem.* **2011**, *35*, 833–841.
100. Manna, S.C.; Konar, S.; Zangrando, E.; Okamoto, K.-I.; Ribas, J.; Chaudhuri, N.R. Mn^{II}/Co^{II}-terephthalate frameworks containing dipyridine coligands: Syntheses, crystal structures, magnetic behaviors, and thermal studies. *Eur. J. Inorg. Chem.* **2005**, *2005*, 4646–4654.
101. Li, J.-X.; Guo, W.-B.; Du, Z.-X.; Huang, W.-P. Monometallic nickel and bimetallic nickel-europium complexes based on oxydiacetic acid and N-heterocyclic ligands. *Inorg. Chim. Acta* **2011**, *375*, 290–297.
102. Manna, S.C.; Ghosh, A.K.; Ribas, J.; Drew, M.G.; Lind, C.N.; Zangrando, E.; Chaudhuri, N.R. Synthesis, crystal structure, magnetic behavior and thermal property of three polynuclear complexes: $[M(dca)_2(H_2O)_2]_n\cdot(hmt)_n$ [M = Mn(II), Co(II)] and $[Co(dca)_2(bpds)]_n$ [dca, dicyanamide; hmt, hexamethylenetetramine; bpds, 4,4′-bipyridyl disulfide]. *Inorg. Chim. Acta* **2006**, *359*, 1395–1403.
103. Saha, R.; Biswas, S.; Mostafa, G. pH-triggered construction of NLO active CMOFs: Change in supramolecular assembly, water clusters, helical architectures and their properties. *CrystEngComm* **2011**, *13*, 1018–1028.
104. Marin, G.; Andruh, M.; Madalan, A.M.; Blake, A.J.; Wilson, C.; Champness, N.R.; Schröder, M. Structural diversity in metal-organic frameworks derived from binuclear alkoxo-bridged copper(II) nodes and pyridyl linkers. *Cryst. Growth Des.* **2008**, *8*, 964–975.